

AD-A222 095

WRDC-TR-89-4138



## X-RAY COMPUTED TOMOGRAPHY OF CASTINGS

Richard H. Bossi  
John L. Cline  
Edward G. Costello  
Benjamin W. Knutson

Boeing Aerospace & Electronics  
P.O. Box 3999  
Seattle, WA 98124-2499

March 1990

Interim Report for Period April 1989 - September 1989

Approved for public release; distribution is unlimited

DTIC  
ELECTE  
MAY 30 1990  
S B D

MATERIALS LABORATORY  
WRIGHT RESEARCH AND DEVELOPMENT CENTER  
AIR FORCE SYSTEMS COMMAND  
WRIGHT-PATTERSON AIR FORCE BASE, OH 45433-6533

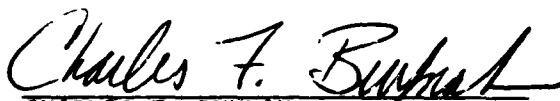
90 05 29 053

## NOTICE

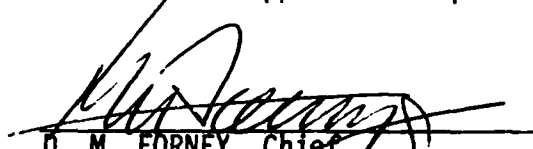
When Government drawings, specifications, or other data are used for any purpose other than in connection with a definitely Government-related procurement, the United States Government incurs no responsibility or any obligation whatsoever. The fact that the Government may have formulated or in any way supplied the said drawings, specifications, or other data, is not to be regarded by implication, or otherwise in any manner construed, as licensing the holder, or any other person or corporation; or as conveying any rights or permission to manufacture, use, or sell any patented invention that may in any way be related thereto.

This report is releasable to the National Technical Information Service (NTIS). At NTIS, it will be available to the general public, including foreign nations.

This technical report has been reviewed and is approved for publication.




CHARLES F. BUYNAK  
Nondestructive Evaluation Branch  
Metals and Ceramics Division



D. M. FORNEY, Chief  
Nondestructive Evaluation Branch  
Metals and Ceramics Division

FOR THE COMMANDER



DR. NORMAN M. TALLAN, Director  
Metals and Ceramics Division  
Materials Laboratory

If your address has changed, if you wish to be removed from our mailing list, or if the addressee is no longer employed by your organization please notify WRDC/MLLP, Wright-Patterson AFB, OH 45433-6533 to help us maintain a current mailing list.

Copies of this report should not be returned unless return is required by security considerations, contractual obligations, or notice on a specific document.

## REPORT DOCUMENTATION PAGE

Form Approved  
OMB No. 0704-0188

1a. REPORT SECURITY CLASSIFICATION UNCLASSIFIED			1b. RESTRICTIVE MARKINGS		
2a. SECURITY CLASSIFICATION AUTHORITY			3. DISTRIBUTION / AVAILABILITY OF REPORT  APPROVED FOR PUBLIC RELEASE DISTRIBUTION IS UNLIMITED		
2b. DECLASSIFICATION / DOWNGRADING SCHEDULE			5. MONITORING ORGANIZATION REPORT NUMBER(S) WRDC-TR-89-4138		
4. PERFORMING ORGANIZATION REPORT NUMBER(S)			7a. NAME OF MONITORING ORGANIZATION WRIGHT RESEARCH & DEVELOPMENT CENTER MATERIALS LABORATORY (WRDC/MLLP)		
6a. NAME OF PERFORMING ORGANIZATION Boeing Aerospace & Electronics		6b. OFFICE SYMBOL (If applicable)		7b. ADDRESS (City, State, and ZIP Code) WRIGHT PATTERSON AFB, OH 45433-6533	
6c. ADDRESS (City, State, and ZIP Code) P.O. Box 3999 Seattle, WA 98124-2499			9. PROCUREMENT INSTRUMENT IDENTIFICATION NUMBER F33615-88-C-5404		
8a. NAME OF FUNDING / SPONSORING ORGANIZATION		8b. OFFICE SYMBOL (If applicable)		10. SOURCE OF FUNDING NUMBERS	
8c. ADDRESS (City, State, and ZIP Code)		PROGRAM ELEMENT NO. 63211F		PROJECT NO. 3153	WORK UNIT ACCESSION NO. 06
11. TITLE (Include Security Classification) X-RAY COMPUTED TOMOGRAPHY OF CASTINGS					
12. PERSONAL AUTHOR(S) JOHN L. CLYNE AND RICHARD H. BOSSI					
13a. TYPE OF REPORT INTERIM		13b. TIME COVERED FROM APR 89 TO SEP 89		14. DATE OF REPORT (Year, Month, Day) March 1990	
15. PAGE COUNT 60					
16. SUPPLEMENTARY NOTATION					
17. COSATI CODES			18. SUBJECT TERMS (Continue on reverse if necessary and identify by block number)		
FIELD	GROUP	SUB-GROUP	Castings, /X-ray /Shrinkage Computed Tomography, (CT) /Radiography, (RAD) (YES) ✓ Nondestructive Evaluation, (NDE) /Inspection/Contract (Cont)		
11	06				
11	03				
19. ABSTRACT (Continue on reverse if necessary and identify by block number)  Computed Tomography (CT) offers an inspection capability with potential to overcome some of the shortcomings in inspection which affect the utilization of castings in the aircraft/aerospace industry. To this end, castings defect samples were excised from larger cast parts and utilized to evaluate CT sensitivity to a variety of defect types and sizes relative to conventional film radiography. The defects were also inserted into larger cast structures to evaluate loss of sensitivity as a function of geometry. Dimensional phantoms were fabricated to test dimensional measurement accuracy of CT systems. Five different CT systems were used for the CT scanning. Data from resolution and contrast sensitivity phantoms, developed for the program, were used to establish quantitative measures of imaging capability.  (Con't)					
20. DISTRIBUTION / AVAILABILITY OF ABSTRACT <input checked="" type="checkbox"/> UNCLASSIFIED/UNLIMITED <input type="checkbox"/> SAME AS RPT. <input type="checkbox"/> DTIC USERS			21. ABSTRACT SECURITY CLASSIFICATION UNCLASSIFIED		
22a. NAME OF RESPONSIBLE INDIVIDUAL Charles F. Buynak			22b. TELEPHONE (Include Area Code) 59802		22c. OFFICE SYMBOL WRDC/MLLP

18. (Con't)  
Density Phantom  
Contrast Phantom

19. (Con't)

The results of the preliminary testing on castings shows that CT has excellent sensitivity to casting defects. CT systems with 2 to 4 lp/mm resolution can readily image ASTM F2 level holes and porosity in test coupons with superior detail sensitivity to film radiography. The use of volumetric data sets to create three-dimensional models of flaws is very effective for visualization of casting defects. CT dimensional measurements with excellent accuracy and precision better than 50 microns (0.002 inches) were demonstrated on test phantoms. As casting size and geometry complexity is increased the CT sensitivity and measurement accuracy is reduced. The quantification of this sensitivity loss and the cost of CT system modification to overcome it are tradeoff factors that affect the overall economic evaluation of CT for castings. These issues could not be fully addressed in this task assignment.

The concern of manufacturing engineers on the validity of current inspection practice for casting acceptance indicates that the quantitative, three-dimensional CT data will be extremely valuable for new casting and production inspection. The economic return for CT is expected to be in terms of increasing casting reliability and reducing unnecessary rejection of product. To achieve these economic returns further testing on full-scale castings is needed. It is recommended that preliminary CT testing be pursued to quantify the detection sensitivity and measurement accuracies possible on full-scale castings, and to establish the economic factors for CT system performance necessary to meet inspection requirements.



## TABLE OF CONTENTS

Section	Page
1.0 INTRODUCTION	1
1.1 Scope	1
1.2 Objectives	1
1.3 NDE of Castings	2
1.3.1 Film Radiography	2
1.3.2 Computed Tomography	5
2.0 TEST PLAN	6
2.1 Part Selection	6
2.2 Performance Characteristics	6
3.0 COMPONENT TESTING AND RESULTS	9
3.1 CT Correlation to RT Test Results	9
3.1.1 Filamentary Shrinkage, PID #119	10
3.1.2 Dendritic Shrinkage, PID #132	10
3.1.3 Shrinkage Holes, PID #125	10
3.1.4 Porosity, PID #115	16
3.1.5 Shrinkage Holes, PID #118A	16
3.1.6 Surface Crack, PID #120	16
3.2 Full-Scale Parts	20
3.2.1 Inlet Duct Casting, PID #127	20
3.2.2 Handle-Box Casting, PID #102	20
3.3 Dimensional Measurements	25
3.3.1 Aluminum Dimension Phantom, PID #000801	25
3.3.2 Steel Dimension Phantom, PID #000701	28
3.4 Three Dimensional Results	28
4.0 COST BENEFIT ANALYSIS	32
4.1 On-line Inspection of Castings	32
4.2 Performance Engineering Evaluation	33
4.3 New Product Development/First Article Inspection	34
4.4 Standards	34
5.0 CONCLUSIONS AND RECOMMENDATIONS	36
5.1 CT of Castings Conclusions	36
5.2 Recommendations	37
6.0 REFERENCES	38



### APPENDICES

- A: X-RAY IMAGING TECHNIQUES
- B: FOUNDRY CONTACT LIST
- C: CT PHANTOMS

<b>Accession For</b>	
NTIS GRA&I	<input checked="" type="checkbox"/>
DTIC TAB	<input type="checkbox"/>
Unannounced	<input type="checkbox"/>
Justification	
By _____	
Distribution/	
Availability Codes	
Dist	Avail and/or Special
A-1	

39  
42  
45

## LIST OF FIGURES

Figure		Page
1.3-1	ASTM standard flaw levels for gas holes in aluminum	3
1.3-2	ASTM standard flaw levels for shrinkage in aluminum	4
2.1-1	Castings description	7
2.2-1	CT systems performance chart	8
3.1-1	CT correlation to RT	9
3.1-2	PID #119, filamentary shrinkage	11
3.1-3	CT scans of PID #119, filamentary shrinkage	12
3.1-4	PID #132, dendritic (feather ) shrinkage	13
3.1-5	PID #125, shrinkage holes	14
3.1-6	CT scans of PID #125, shrinkage holes	15
3.1-7	PID #115, porosity (gas bubbles)	17
3.1-8	PID #118A, shrinkage holes	18
3.1-9	PID #120, 0.5 mm surface cracks	19
3.2-1	Full-scale castings	21
3.2-2	CT scans of PID #118A, alone and inserted in inlet duct casting, showing shrinkage holes	22
3.2-3	CT scans of PID #120 alone and inserted in inlet duct casting	23
3.2-4	PID #118A and #120 inserted in handle-box casting	24
3.3-1	Aluminum dimensional phantom CT scan from System J	26
3.3-2	Results of dimensional measurements	26
3.3-3	Line plot traces across aluminum dimensional phantom gaps, System J	27
3.3-4	Crossover percentage vs gap width	27
3.3-5	Steel dimensional phantom results	29
3.4-1	Two selected 3D views of PID #119 (shrinkage)	30
3.4-2	Two selected 3D views of PID #118A (holes)	30
3.4-3	Two selected 3D views of PID #120 (crack)	30
3.4-4	PID #502, steel elbow casting	31
A1-1	Film radiography	39
A2-1	Digital radiography	40
A3-1	Computed tomography	41
C1-1	Photo of resolution phantom	46
C1-2	CT slice taken on the resolution phantom	46
C2-1	CT slice of contrast sensitivity phantom	48
C3-1	Density calibration phantom	49
C3-2	CT scan of density calibration phantom	50
C3-3	Calibration plot	50
C4-1	Aluminum dimensional phantom	51
C4-2	Photo of aluminum dimensional phantom	51
C4-3	Line trace across 1 mm gap from a CT image	51
C5-1	Steel dimensional phantom	53
C5-2	Photo of steel dimensional phantom	53
C5-3	Line trace across spoke with two 3.8 mm walls	53

## DISCLAIMER

The information contained in this document is neither an endorsement nor criticism for any X-ray imaging instrumentation or equipment used in this study.

## 1.0 INTRODUCTION

The goal of the Advanced Development of X-Ray Computed Tomography Applications demonstration (CTAD) program is to evaluate inspection applications for which computed tomography (CT) can provide a cost-effective means of inspecting aircraft/aerospace components. The program is task assigned so that specific CT applications or application areas can be addressed in separate task assigned projects. This interim report is the result of a task assignment study. Under the program, candidate hardware is selected for testing that offers potential for return on investment (ROI) for the nondestructive evaluation system and operation. Three categories of task assignment are employed in the program: 1) preliminary tests where a variety of parts and components in an application area are evaluated for their suitability to CT examinations for their inspection; 2) final tests where one or a few components are selected for detailed testing of CT capability to detect and quantify defects; and 3) demonstrations where the economic viability of CT to the inspection problem are analyzed and the results presented to government and industry.

X-ray computed tomography (CT) is a powerful nondestructive evaluation technique that was conceived in the early 1960's and has been developing rapidly ever since. CT uses penetrating radiation from many angles to reconstruct image cross sections of an object. The clear images of an interior plane of an object are achieved without the confusion of superposition of features often found with conventional film radiography. CT can provide quantitative information about the density and dimensions of the features imaged.

Although CT has been predominantly applied to medical diagnosis, industrial applications have been growing over the past decade. Medical systems are designed for high throughput and low dosages specifically for humans and human sized objects. These systems can be applied to industrial objects that have low atomic number and are less than one-half meter in diameter. Industrial CT systems do not have dosage and size constraints. They are built in a wide range of sizes from the inspection of small jet engine turbine blades using mid-energy (hundreds of keV) X-ray sources to the inspection of large ICBM missiles requiring high (MeV level) X-ray energies. Industrial CT systems generally have much less throughput than medical systems. The CTAD program utilizes a wide range of CT systems, both medical and industrial.

### 1.1 Scope

This task assignment, designated "Task 3 - Castings", is a preliminary testing task in the area of aircraft/aerospace castings. This report discusses the components selected for CT testing, the results of testing, the implications of the results for economic application of CT to castings and recommendations for future direction.

### 1.2 Objectives

The overall program goal is to evaluate the economic incentive to utilize CT in the aircraft/aerospace industry. The objective for this task assignment was to identify the applicability and economic potential of CT for the inspection of castings. The casting industry has well established inspection practices, but they have severe limitations and economic impact on the use of castings. CT offers a different inspection orientation and data analysis capability from film radiography. It offers considerable potential to overcome some of the limitations of current practice. Because there is no established criteria for CT inspection of castings, it was necessary in this preliminary task assignment to correlate CT data to conventional film radiographic inspection criteria.

The approach to evaluate CT applicability to castings was to obtain various casting defects and compare the capability of CT with conventional radiography for defect characterization. The dimensional measurement accuracy of CT and the effect of full-scale casting geometry on the CT inspection sensitivity were also addressed.

### 1.3 NDE of Castings

Castings are used extensively in the aircraft and aerospace industry and include aluminum, magnesium, titanium and steel alloys. Compared to forgings and billet machined parts they are far less expensive by approximately a factor of four. Castings can be produced in complicated shapes that are impossible with machining techniques. Most castings contain imperfections to some degree; some are serious. Surface flaws are detected using visual and dye penetrant inspection. Subsurface flaws are detected with radiographic inspection.

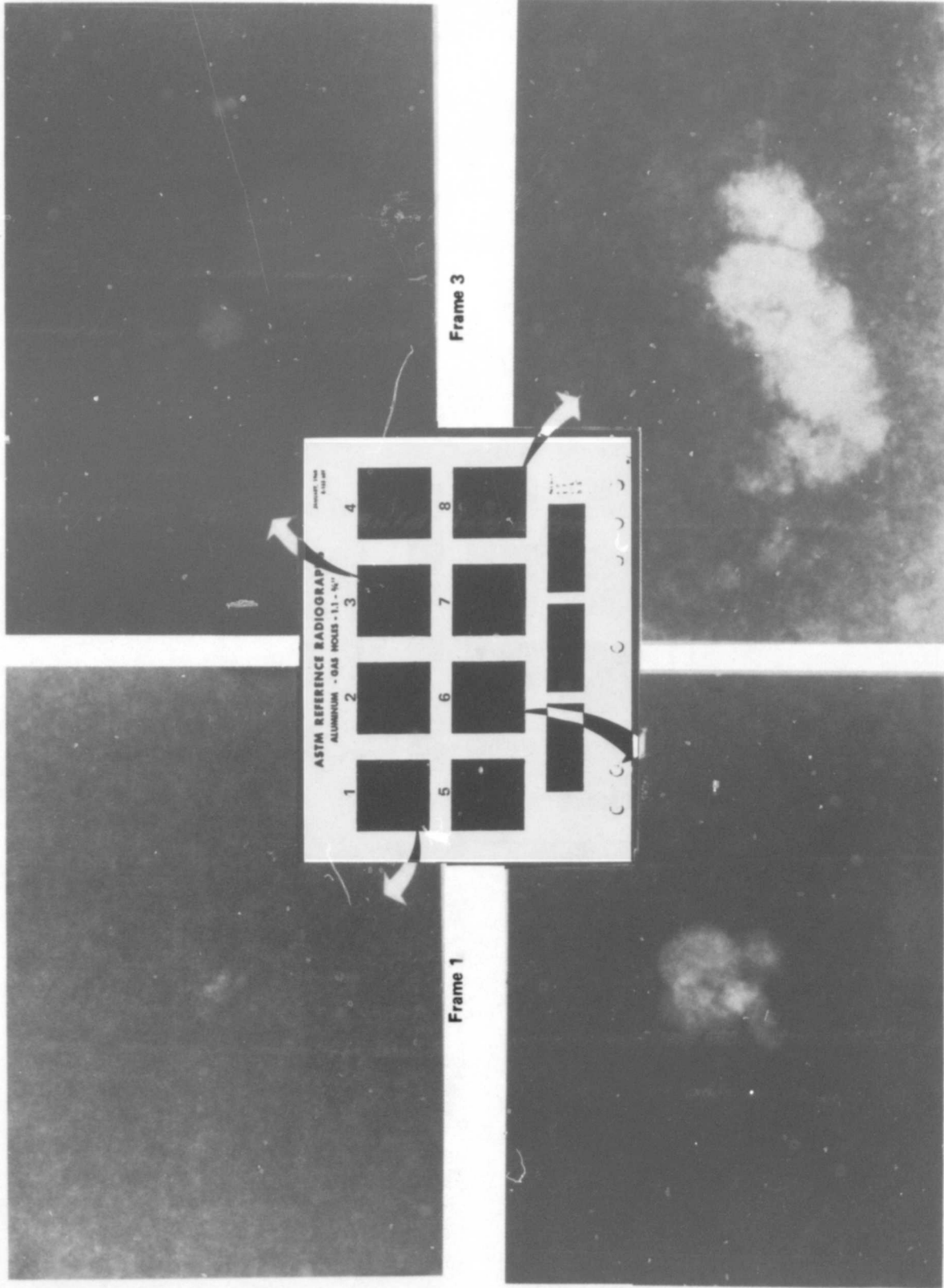
Three X-ray imaging techniques are addressed in this report: film radiography (RT), digital radiography (DR) and computed tomography (CT). A description of each of these techniques is given in Appendix A.

#### 1.3.1 Film Radiography

The radiographic (film X-ray) inspection of castings for imperfections such as gas holes, porosity, shrinkage, inclusions and cracks is performed routinely in the aerospace industry. In current inspection practice, the casting radiograph is compared to ASTM reference radiographs and a judgement is made on the defect level. A category (F1 to F8), ranging in increasing order of severity, is assigned. In the case of aluminum castings, the ASTM E155-60T reference radiographs include sets of radiographs at two aluminum thicknesses, 6.4 mm (0.25 inch) and 19 mm (0.75 inch), for gas holes, gas porosity (round), gas porosity (elongated), shrinkage (sponge), shrinkage (cavity), foreign material (less dense), and foreign material (more dense). The 6.4 mm (0.25 inch) standard set is used for parts up to 12.5 mm (0.5 inch) thick and the 19 mm (0.75 inch) standard set is used for parts greater than 12.5 mm (0.5 inch) and up to 50 mm (2 inch) thick. Figures 1.3-1 and Figure 1.3-2 show X-ray film reproductions of casting flaws taken from the ASTM E155-60T reference radiograph set. Figures 1.3-1 shows frames 1, 3, 6, and 8 level of aluminum gas holes and Figure 1.3-2 shows frames 1, 3, 6, and 8 level of aluminum shrinkage cavities.

Once the part is radiographed the film is reviewed and the ASTM reference frame number value is assigned. The part is accepted or rejected based on the design allowable flaw levels (F1 to F8 for porosity, shrinkage, holes, etc.) for that part. In the case of cracks, any discernable crack indication in the casting radiograph is considered sufficient cause for rejection. There are a number of shortcomings to this evaluation. The primary problem is that the ASTM standard is responsive to the capability of film radiography, not the engineering requirement on the casting performance.

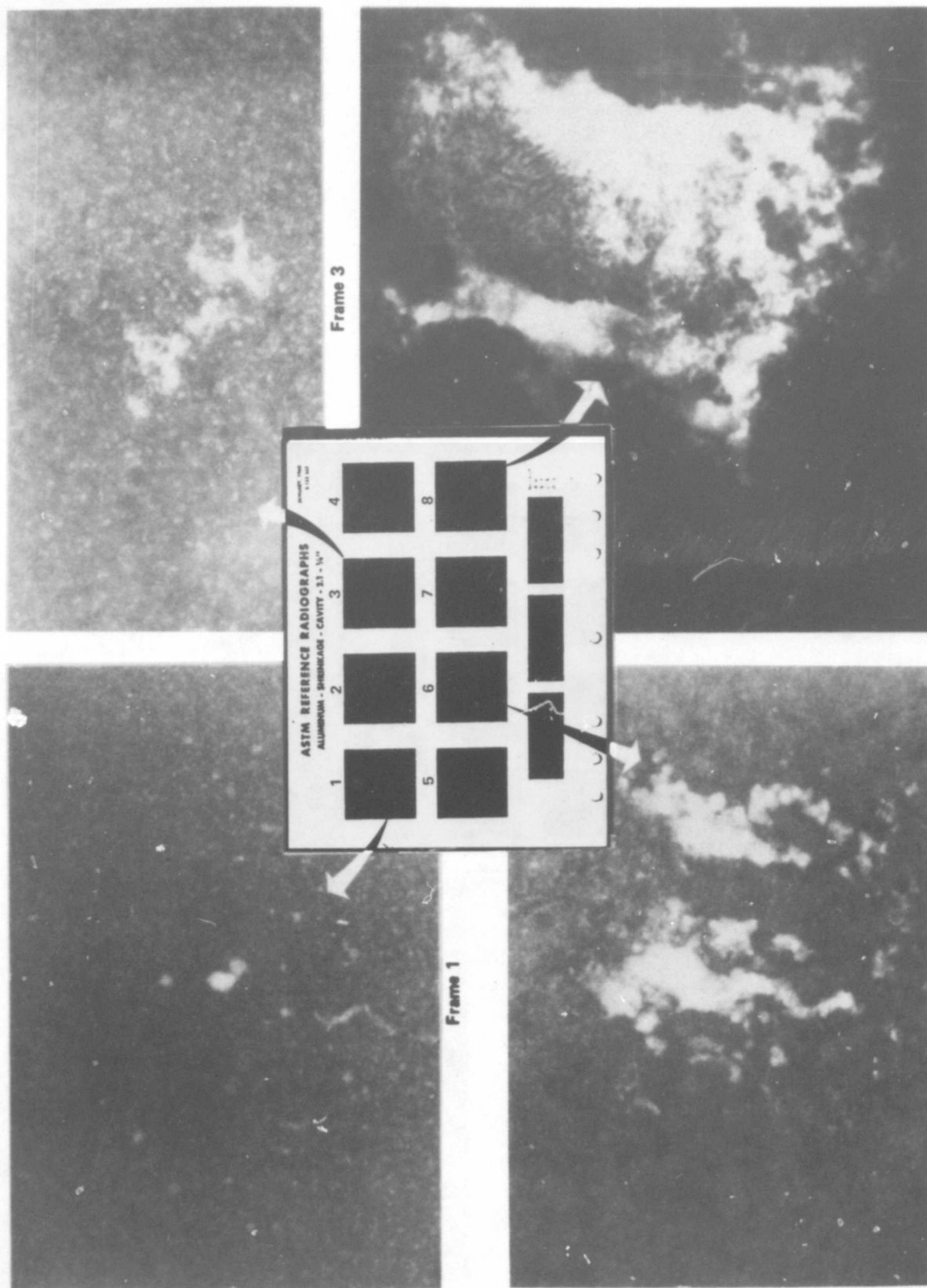
The interpretation of flaw severity by film radiography is subjective and may vary widely between independent radiographers. In addition, the thickness of the part influences the detectability of flaws. A radiograph of a thicker part with the same flaw condition as a thinner part will produce a lower contrast image. Interpretation of radiographs is often compromised by surface features or irregularities which may give false appearances of non-existent flaws. The depth and distribution of flaws cannot be known from a single radiograph due to the lack of three-dimensional information. Also, film radiography may provide little or no useful information in critical inspection areas because of the difficulty of film placement and X-ray beam orientation on specimens of unusual geometry, i.e., complex shape, thickness or curvature. Because RT cannot



Frame 6

Figure 1.3-1 ASTM standard flaw levels for gas holes in aluminum

Frame 8



Frame 8

Frame 6

Figure 1.3-2 ASTM standard flaw levels for shrinkage in aluminum

Frame 1

Frame 3

precisely define flaw size and location throughout a complex part, the acceptance criteria must be extremely conservative, often resulting in the rejection of useful product.

### 1.3.2 Computed Tomography (CT)

CT provides better flaw depth and flaw distribution information than conventional RT. The superposition of information in RT, which reduces sensitivity, is eliminated in CT scanning. CT can precisely define the size and location of shrinkage, holes, porosity and cracks within the inspected component. Depth information is useful in categorizing and evaluating defects. Because complete spatial information on part configuration and defect location is available from CT, an engineering assessment of fitness-for-service of the as-built component is possible which could potentially reduce casting rejections significantly.

Digital radiography is a companion feature on CT systems and provides very similar information to film radiography. DR scans are commonly used to identify the CT slice plane location(s) prior to performing CT scans at those selected elevations on the component. Both CT and DR result in digital data sets that can be readily processed by image processing software for display and enhancement.

## **2.0 TEST PLAN**

### **2.1 Part Selection**

Casting defect samples of various types were sought from the aircraft/aerospace industry for studying CT capability. Contacts were made with numerous foundries. A listing of the foundries and type of castings they manufacture is contained in Appendix B. Figure 2.1-1 is a listing of the casting candidates considered for scanning. The list includes the part identification number assigned for the program and the description of the flaw with ASTM frame number where appropriate. The castings were RT inspected and the film evaluation was used to select those

In order to compare the detectability of RT and CT on casting defects in a controlled manner, the flawed area was excised from the original host structure in a number of the samples. This process resulted in small test specimens which typically averaged about 40 mm. (1.6 inches) in diameter and 5 to 25 mm (0.2 to 1 inch) in thickness. The excised coupons contained documented flaws, i.e., shrinkage, holes/porosity and cracks, ranging in severity from ASTM F2 to F8. Larger casting samples were also maintained for evaluation of the effect of detectability of defects when inserted in the large structure format.

### **2.2 Performance Characteristics**

Two high resolution (2 to 4 lp/mm - GE Bench XIM, SMS CITA 101B) and two medium resolution (1 lp/mm - ARACOR ARNIS I (Aerojet), Bioluming ACTIS (Boeing)) industrial CT systems, and one medical CT system (GE CT9800 QUIK) were evaluated for their performance. Figure 2.2-1 lists the performance characteristics of the CT systems measured on this task assignment. The measurements were obtained using the resolution and noise test phantoms described in Appendix C. The CT systems are designated in Figure 2.2-1 by an arbitrary lettering assignment that has been used throughout the CTAD program [1,2]. CT images discussed in the report can be correlated to the resolution and contrast sensitivity capability of the CT system utilized by reference to this figure. This data is useful for establishing the CT performance level necessary to achieve inspection goals.

The CT images selected for reproduction in this report are examples of the quality that can be achieved by utilizing a CT system having similar imaging capability. Due to the reproduction process, however, the image quality is less than that observed in the original data on the image display system.

In addition to the resolution, noise and density phantoms used to measure CT system characteristics, dimensional measurement phantoms were developed for this task assignment and are also described in Appendix C. The use of these phantoms is discussed in Section 3.3.



PID #	Description	Defect Type	ASTM Frame #
<b>A. Sandcastings, Aluminum - Aircraft</b>			
030115A	Coupon	Surface porosity	F6
030115B	Coupon	Surface porosity	F5
030116	Coupon	Large porosity	F4
030117	Coupon	Mult. holes	-
030118A	Coupon	Mult. holes	F5-F6
030118B	Coupon	Porosity	F1
030119	Coupon	String LDI	-
030120	Coupon	Surface Cracks	*
030121	Coupon	Spot in this area	F3
030122	Coupon	Large hole	F3
030123	Coupon	Porosity w/lg.hole	F1,F2
030124	Coupon	Small edge crack	*
030125	Coupon	Multiple Holes	F7-F8
030126	Main Inlet Duct No. 1	No obvious RT ind.	F1 or less
030127	Main Inlet Duct No. 2	Surface Hole	F8
030128	Air Inlet Scoop	No obvious RT ind.	F1 or less
030129	Triangle Plate	No obvious RT ind.	F1 or less
030130	Thick Rectangle	Small Crack/Shrink	*
030131	Thick Plate	Porosity	F2
<b>B. Sandcastings, Aluminum - Missile</b>			
030132	Thick Rectangle	Shrink	F8
030133	Thick Plate	Shrink	F5
030134	Thick Plate	Shrink	F4-F8
030135	Triangle Knob	Shrink	F1 or less
030136	Thin Wall Plate	Surface flaw	F2
030137	Small Thick Rectangular	Shrink	F4
030138	Thick Square	Shrink	F5
030139	Full Web	Shrink	F2-F3
<b>C. Magnesium Castings - Aircraft</b>			
030201	Banjo Trim Mechanism.	unknown	
<b>D. Titanium Castings - Aircraft Engines</b>			
030302	Step wedge	Voids & inclusions	—
030303	Blade section	Porosity	—
<b>E. Steel Castings</b>			
030501	Tounge	Shrinkage	F1-F3
030502	Pipe Coupler	Dimensional	F1-F3
030503	"V" Plate	Shrinkage	F1-F3
030504	Adaptor	No obvious RT ind	F1-F3
030505	Collar	Shrinkage	F1-F3

\* Cracks are not given frame numbers

Figure 2.1-1 Castings description

Scan conditions				Results						Signal to noise
System (6)	Energy kV	Slice thickness (mm)	Scan time	Percent modulation						
				FOV (mm)	Std. used	lp/mm				
						0.5	1	2	4	
B	225	0.5	7.5 min 19 min	50 60	Steel Steel	86 92	49 69	5 17	1 5	6:1 (1)
I	2000	6 (4) 10 (5)	4.6 min	440	Steel	13 39	0 2	0 0	0 0	107:1(1)
J	410	0.25	53 sec	152	Steel	84	60	15	1	14:1 (1)
K	120	10	4 sec	100	Al	81	5	0	0	149:1(2) 22:1 (3) —
		10	4 sec	100		81	5	0	0	
		1.5	4 sec	100		79	4	0	0	
L	400	4	16 min	100	Steel	38	10	0	0	100:1 (1)

Notes: (1) Lg Al noise std 5.5"  
(2) Sm Al noise std 2.75"  
(3) Acrylic noise std 5.5"  
(4) 512 reconstruction  
(5) 1024 reconstruction  
(6) Systems identified by arbitrary labels ( ref [1], [2] )

Figure 2.2-1 CT systems performance chart

### 3.0 COMPONENT TESTING AND RESULTS

A primary objective of the preliminary CT testing was to verify the ability of CT to detect defects that are routinely categorized with conventional film radiography. The small excised coupons containing casting defects were used to directly correlate the measurement sensitivity of CT and RT to defect type. Defects in larger components were simulated by inserting the flawed coupon(s) into machined openings in the host structure. The latter condition provided important information regarding the degradation of the CT defect detectability due to the additional material and geometry in the complete casting component.

Only a limited, representative number of test results from the Figure 2.1-1 candidates are presented in this report. Note that in the following testing results, casting components are referenced by the last 3 digits of the part identification (PID) number and that the full PID number for aluminum castings is 030XXX.

#### 3.1 CT Correlation to RT Test Results

A variety of the casting coupons containing holes/porosity, shrinkage and cracks were CT scanned on the systems listed in Figures 2.2-1. The ability of the different CT systems to detect casting defects is shown in Figure 3.1-1. Figure 3.1-1 lists the coupon part identification (PID) number, the ASTM reference frame numbers and whether the defect conditions were detectable by the CT systems tested. These examples were chosen to show a range of ASTM categories. Several of the coupons contained more than one category of defect as determined by film radiography. For the fine defects (F2 range) only the high resolution (2 to 4 lp/mm) CT systems could detect the flaws. As the ASTM frame number increased, the 1 lp/mm systems could also detect the flaws.

PID #	ASTM Frame #	System J	System B	System L	System I	System K
118B	F1-F3	Detectable	Detectable	Not Detectable	Not Detectable	Not Detectable
125	F2	Detectable	Detectable	Detectable	Detectable	Not Detectable
118A	F5-F6	Detectable	Detectable	Detectable	Detectable	Detectable
125	F7-F8	Detectable	Detectable	Detectable	Detectable	Detectable
120	1/2 mm crack	Detectable	Detectable	Detectable	Detectable	Detectable

Figure 3.1-1 CT correlation to RT

Overall, the CT evaluation of the coupons were superior to film radiography and provided essential information on the location of the defect that was not obvious from the radiograph. Specific details of inspections of test coupons containing various defect types, including several of the coupons listed in Figure 3.1-1, are discussed below.

### 3.1.1 Filamentary Shrinkage, PID #119

A small coupon, PID #119, containing multiple string like or filamentary low density indication (LDI) areas caused by shrinkage during solidification of the casting was excised from an aluminum aircraft housing. Figures 3.1-2(a) and (b) are photographs of the full-sized and the excised part. Figure 3.1-2(c) shows two film RT views and Figure 3.1-2(d) shows a DR from System J. Figure 3.1-3(a) through (c) shows three CT slices of the coupon from System J taken at the slice planes indicated in the DR of Figure 3.1-2(d). The filamentary shrinkage area is seen in cross section as string-like low density groupings ranging from 0.25 to 2.0 mm (0.01 to 0.08 inches) in diameter. Figure 3.1-3(d) shows a CT image taken on system K at approximately location CT3. The contrast level setting used in the reproduced image is such that the defect area is observed as an enlarged hole. This system can readily detect the defect feature but does not resolve the detail.

### 3.1.2 Dendritic Shrinkage, PID #132

An example of large shrinkage was found in a sample aluminum casting. The area was excised to form a 170 x 100 x 25 mm (6.7 x 3.9 x 1 inch) slab-like section (PID #132), as shown in Figure 3.1-4(a). The flaws, assigned ASTM F6 - F8 shrinkage, consist of two dendritic (or feathery) shrinkage patterns as shown in the radiograph in Figure 3.1-4 (b). A DR taken on System I is shown in Figure 3.1-4(c). A CT scan normal to the surface, taken on System B, is shown in Figure 3.1-4(d). The CT slice was effective in providing flaw depth and distribution information which is unavailable in the RT or DR images.

Figure 3.1-4(e) shows a thick (15 mm (0.59 inch)) CT scan taken in the plane of the slab-like section on System I using a 2 MV source. The thick CT scan is potentially very useful in quick detection of flaws in a plate. Normally, the thinnest possible CT scan beam is used in CT to provide the highest axial definition. The chief advantage of a single thick slice is that rapid axial coverage can be obtained. It is equivalent to summing together multiple thinner CT slices. Although depth resolution is lost with thicker slices the excellent sensitivity of CT allows fine details to still be detected better than RT (Figure 3.1-4(b) or DR (Figure 3.1-4(c)).

### 3.1.3 Shrinkage Holes, PID #125

An aluminum aircraft sand casting, PID #125, is shown in Figure 3.1-5(a). The area circled on the part contained rejectable flaw material in the form of distributed holes. A film X-ray of the defect region is shown in Figure 3.1-5(b). A square coupon, shown in Figure 3.1-5(c), measuring 38 x 44 x 8 mm (1.5 x 1.7 x 0.3 inches) was excised from the part and milled to remove surface roughness. Holes were discovered in both top and bottom surfaces following machining. The coupon was radiographed and assigned ASTM equivalent frame level areas from F2 to F7 as shown in Figure 3.1-5(d).

A series of four CT images obtained from system J are shown in Figure 3.1-6. The slices were taken near the top surface, in the middle and near the bottom surface of the coupon. The images show that the holes are not evenly distributed through the depth of the coupon. The middle contains multiple small holes visible down to 0.25 mm (0.01 inch) in size. The lighter shade of grey at the edges of the images is the beam hardening artifact common in CT. It is caused by

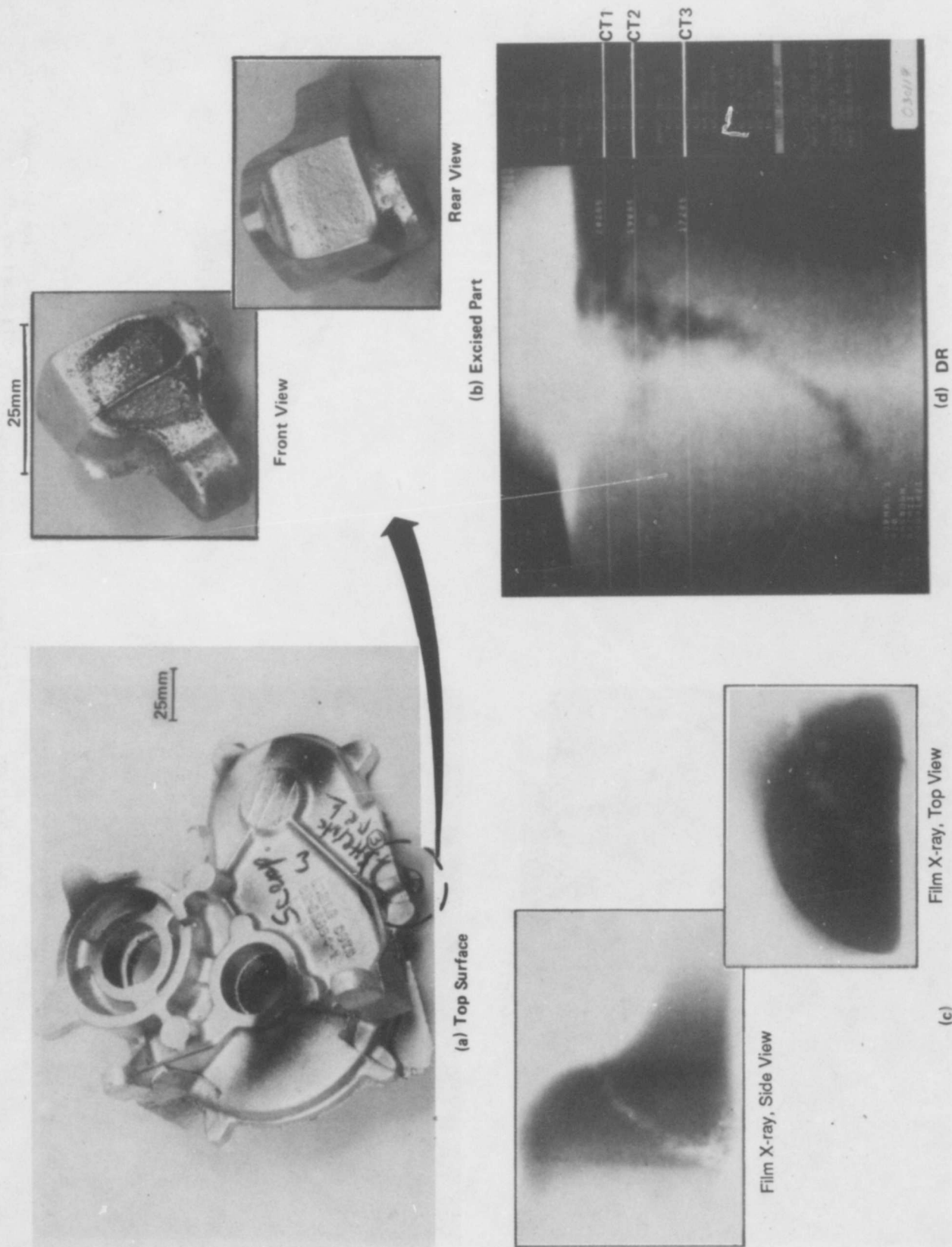
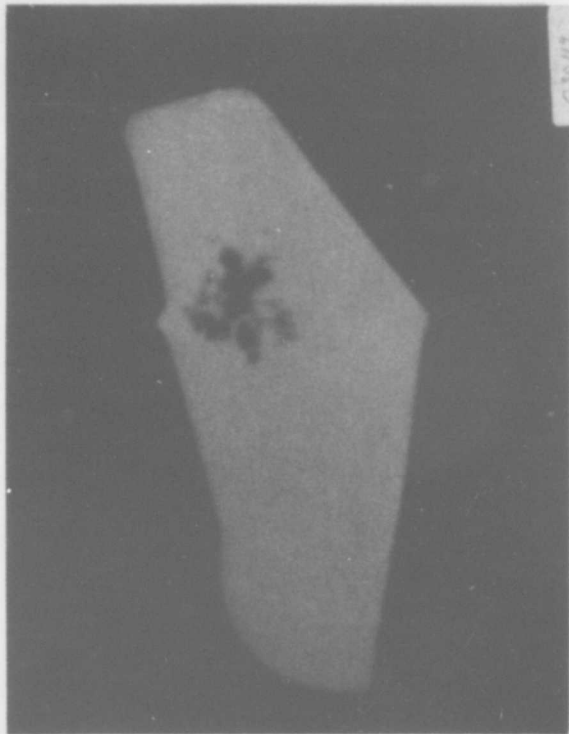


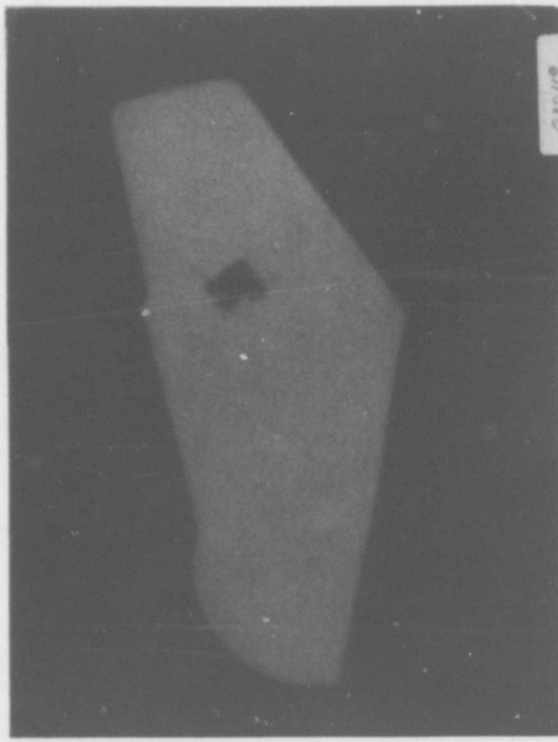
Figure 3.1-2 PID #119, filamentary shrinkage



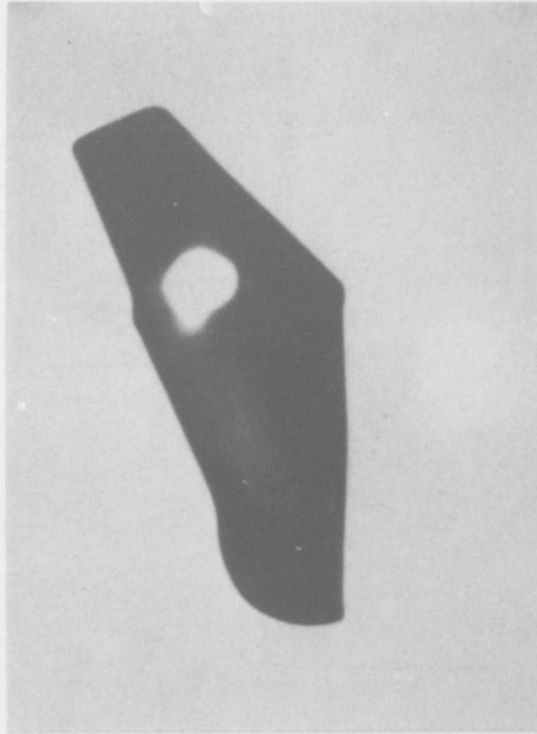
(a) CT1



(b) CT2



(c) CT3



(d) Medical CT Scan (See Figure 3.1-2d.  
CT3 Slice Location)

Figure 3.1-3 CT scans of PID #119, filamentary shrinkage

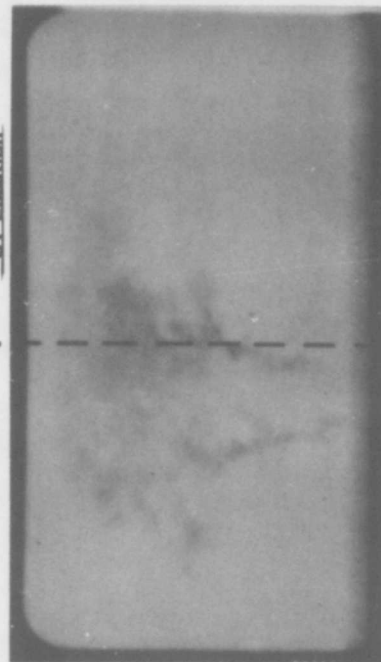


(a) Photo of PID No 132

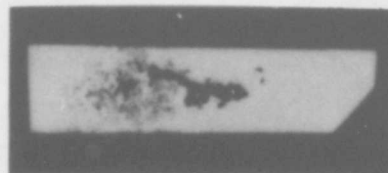


(b) X-Ray

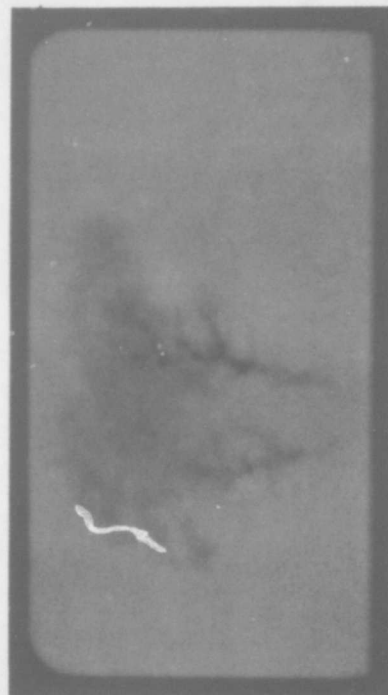
Figure (d)  
CT Location



(c) System I DR



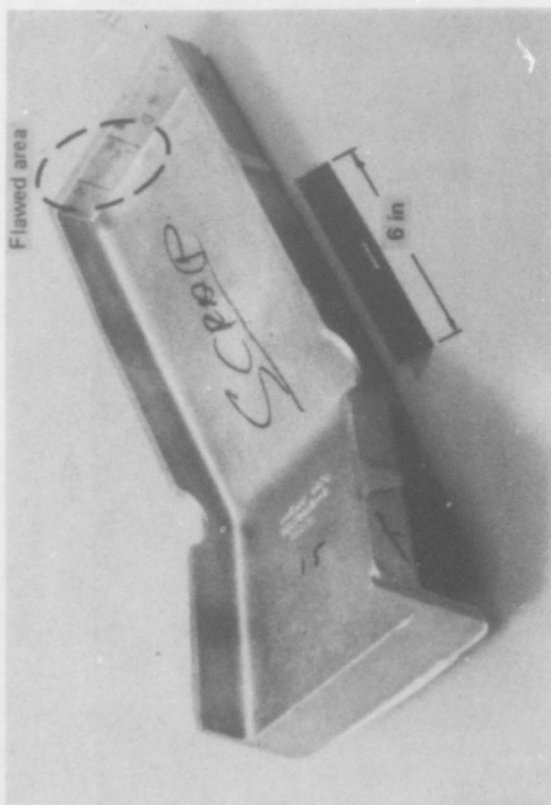
(d) CT Scan as Indicated



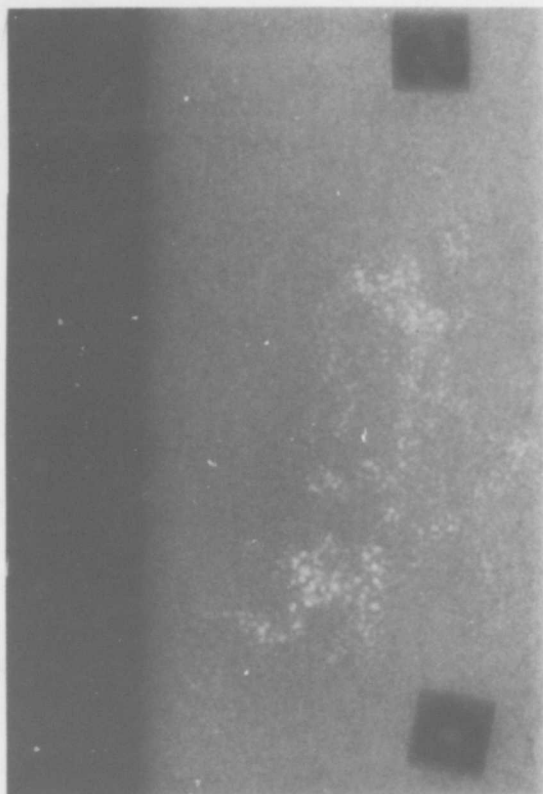
(e) System I Coplaner 15 mm Thick CT Scan

Figure 3.1-4 PID #132, dendritic (feather ) shrinkage

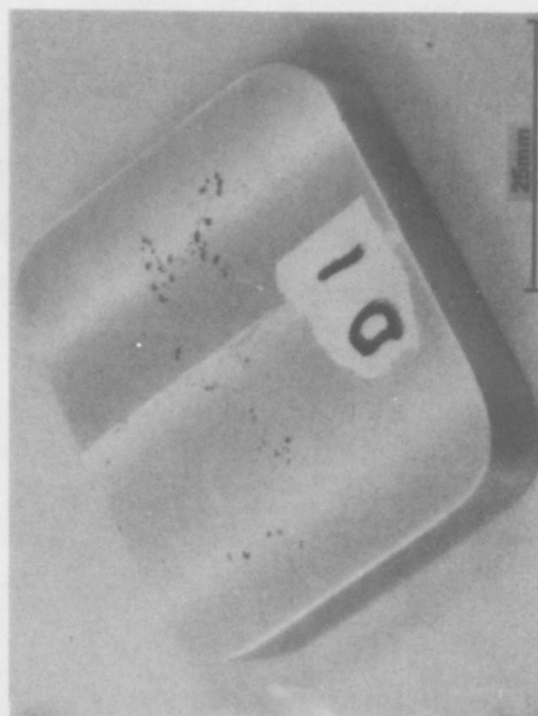




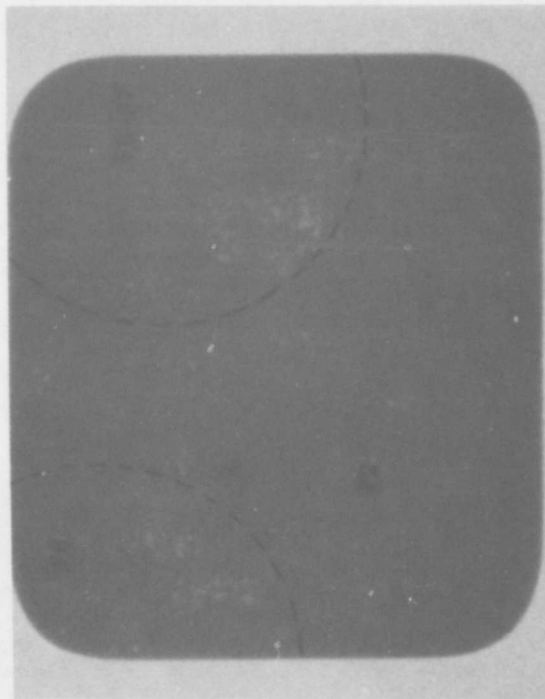
(a) Full Scale Casting



(b) Film X-Ray of Flaw Region



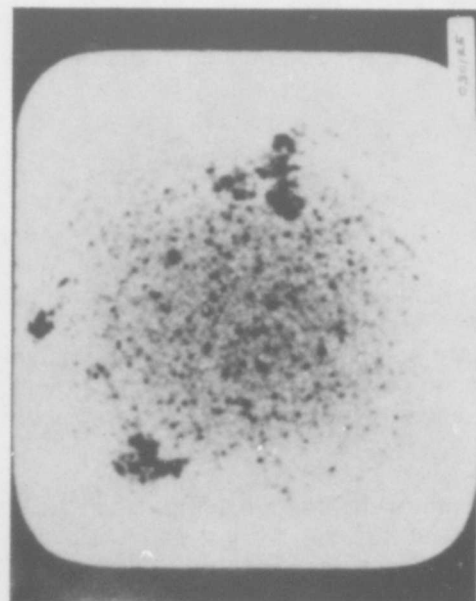
(c) Excised Coupon



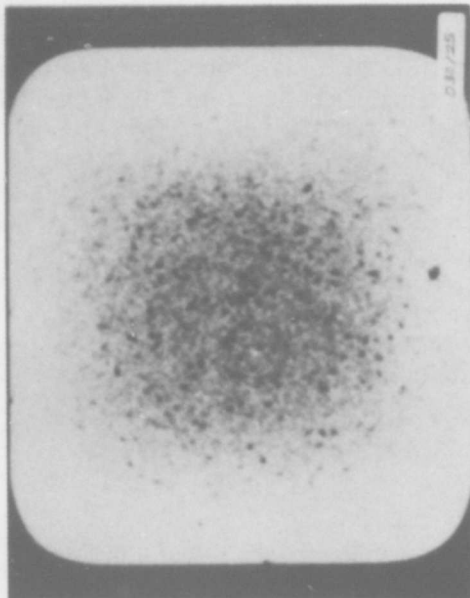
(d) Film X-Ray of Excised Coupon

Figure 3.1-5 PID #125, shrinkage holes

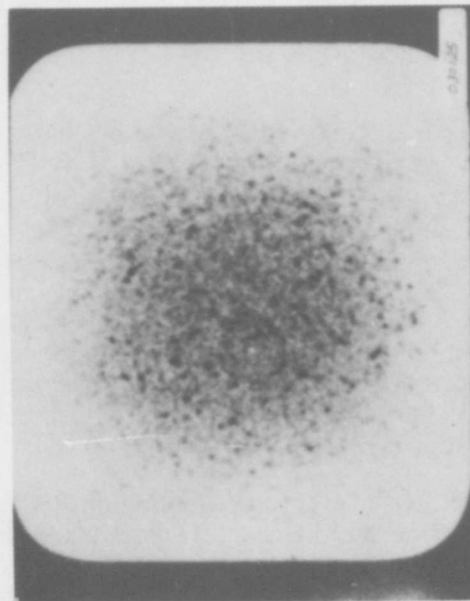




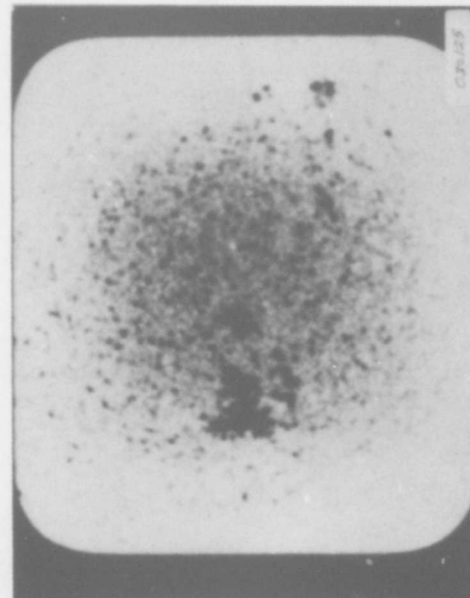
(a) Near Top Surface



(b) Above Center



(c) Below Center



(d) Near Bottom

Figure 3.1-6 CT scans of PID #125, shrinkage holes

selective beam energy absorption of polychromatic X-ray beams along the ray path. Because of the image shading, the contrast level used for reproduction shows feature details in the center of the coupon while washing out features near the edges.

#### 3.1.4 Porosity, PID #115

A curved, thin wall (8 mm (0.3 inch) thick) coupon, PID #115, sectioned from an aluminum aircraft housing containing porosity, is shown in Figure 3.1-7(a). The film RT, Figure 3.1-7(b), of the coupon shows only speckled low density indications rated at ASTM F5-F6 over a 30 mm (0.047 inch) square area. The DR, Figure 3.1-7(c), from System J is comparable to RT. A CT slice across the surface is shown in Figure 3.1-7(d). The CT data shows that the porosity consists primarily of large (up to 0.75 mm (0.03 inch)) distributed gas bubbles near the inside surface. This clear definition of size and location can be extremely useful. The RT and DR images lack depth information of the gas bubbles. The depth information that CT shows indicates that these defects could be readily removed by subsequent machining. Such images are also helpful to casting engineers for understanding the process and altering manufacture to avoid such problems on future parts. Engineers could also use this information to define allowable stress levels for service of this part.

#### 3.1.5 Shrinkage Holes, PID #118A

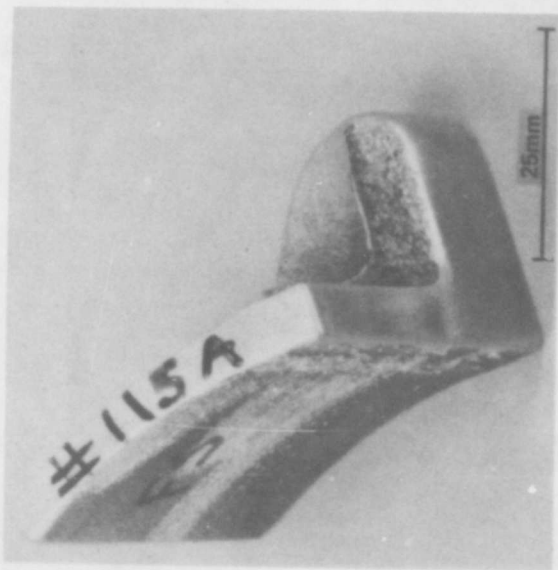
A 40 mm (1.6 inch) diameter defect coupon, PID #118A, excised from a larger aluminum casting, is shown in Figure 3.1-8(a). The RT reproduction shown in Figure 3.1-8(b) indicates that it contains ASTM F5-F6 level holes. The detail of the flaw indications in the RT image are almost blurred out due to the part thickness. Some of the holes can be seen in the photograph of the machined surface of the part, the largest measuring about 0.5 mm (0.02 inches) across.

Figures 3.1-8(c) and (d) are two CT scans taken on system B through the top and lower portions of the coupon, respectively, representing "flawed" and "good" material levels within the coupon. The CT scans clearly indicate that fairly large holes (up to 2 mm (0.08 inch)) exist and are concentrated in the top portion of the coupon. No holes were indicated in the bottom of the coupon.

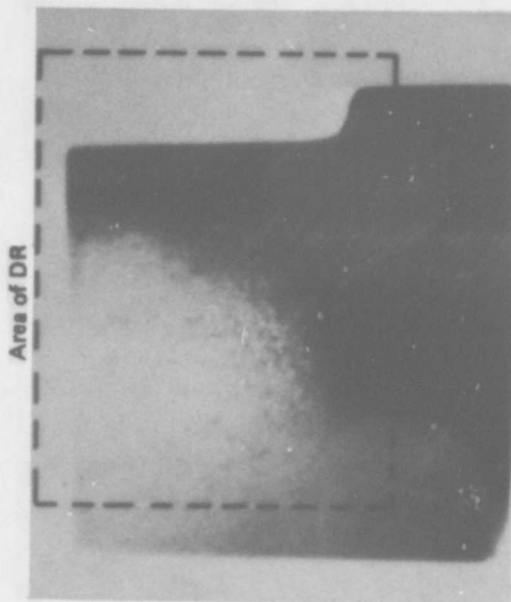
#### 3.1.6 Surface Crack, PID #120

Surface cracks measuring 30 mm (1.2 inches) long and 0.5 mm (0.02 inch) wide were observed in an aluminum sand casting, pictured in Figure 3.1-9(a). A small (42 mm (1.65 inch) diameter x 7 mm (0.28 inch) thick) circular coupon containing the crack was excised from the larger casting for testing. The large shoulder near the crack was removed and the typically rough sand-cast surface was smoothed to eliminate confusing images of surface bumps appearing in the radiograph. The surface on the crack side was not faced off entirely smooth in order to preserve as much of the crack as possible. A slight cleft remained on the coupon as can be seen in the part photograph, Figure 3.1-9(b).

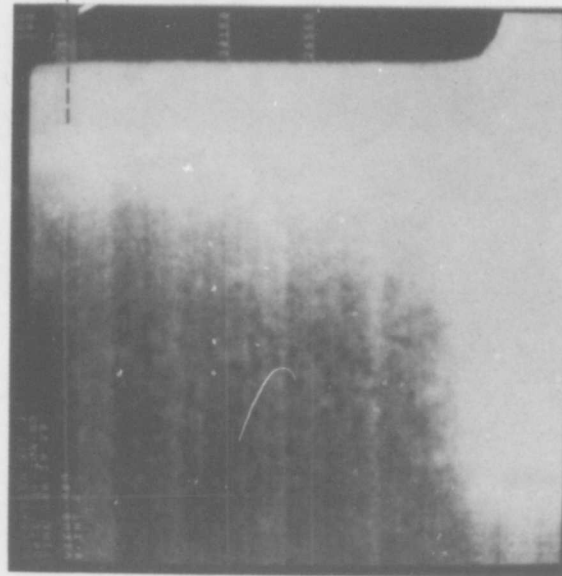
Figure 3.1-9(c) is a reproduction of the film radiograph of the coupon. Figure 3.1-9(d) is a 0.4 mm (0.016 inch) thick CT slice, taken on System B at 225 kV, very near the surface of the coupon. The image shows the near surface holes in the casting. Figure 3.1-9(e) is a CT slice across the part which images the depth of the crack.



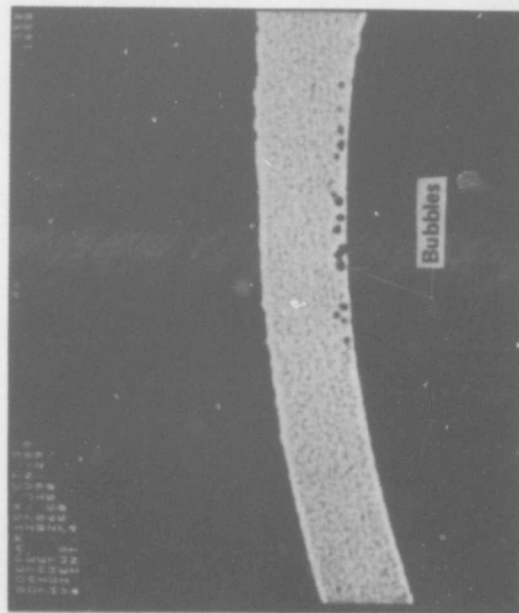
(a) Photo of Coupon



(b) X-Ray

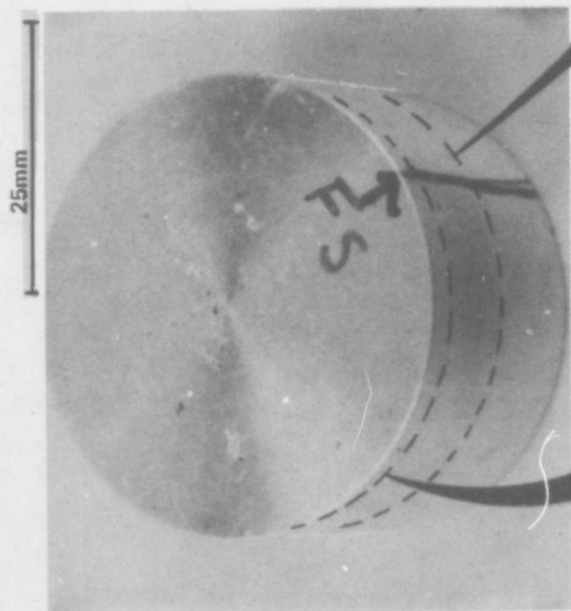


(c) DR (Dotted Section of (b))

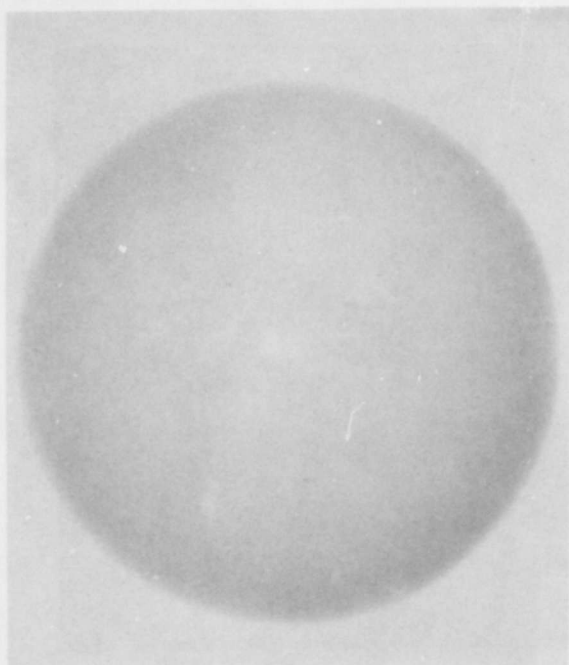


(d) CT Scan Near Top (at 41070 Level)

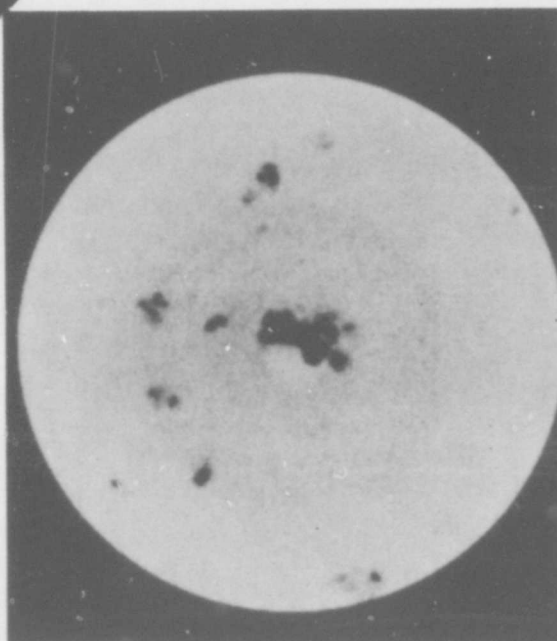
Figure 3.1-7 PID #115, porosity (gas bubbles)



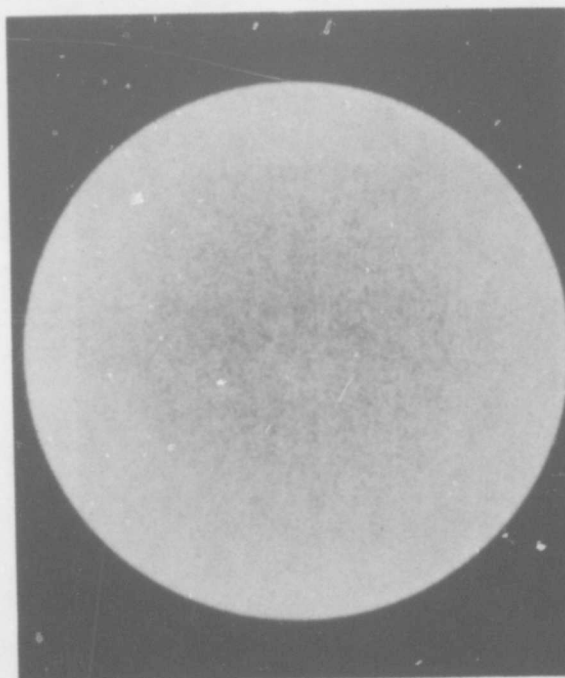
(a) Photo



(b) X-Ray Showing F6-F8 Level Flaws

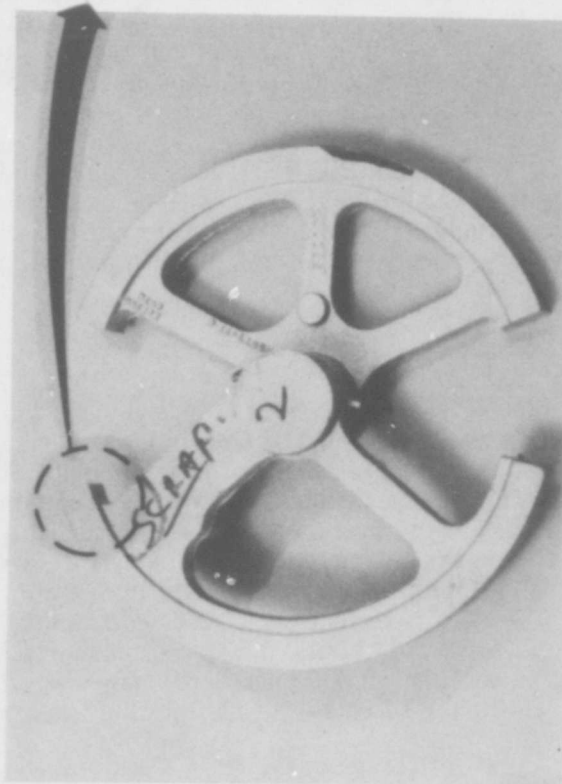


(c) Top Slice Showing Shrinkage Holes

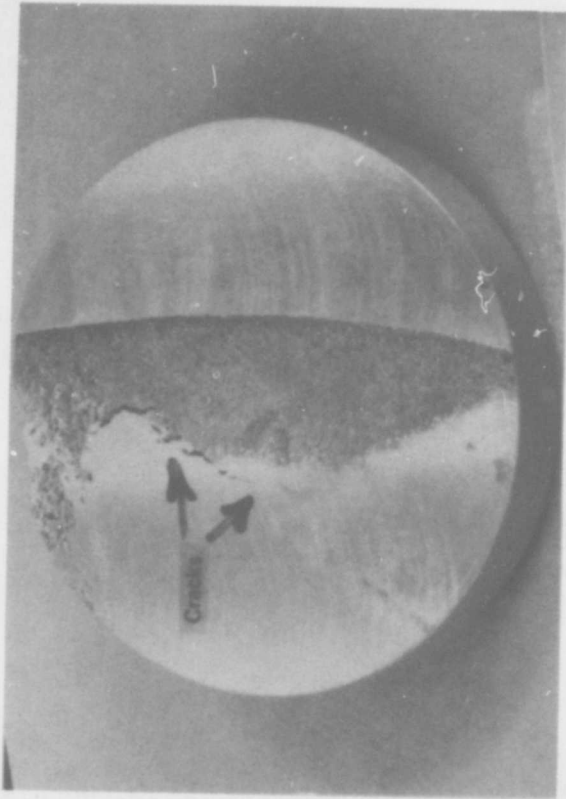


(d) Center Slice 'Good' Area

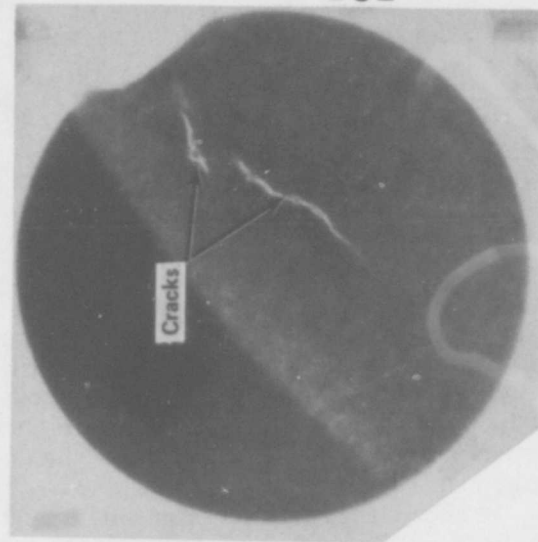
Figure 3.1-8 PID #118A, shrinkage holes



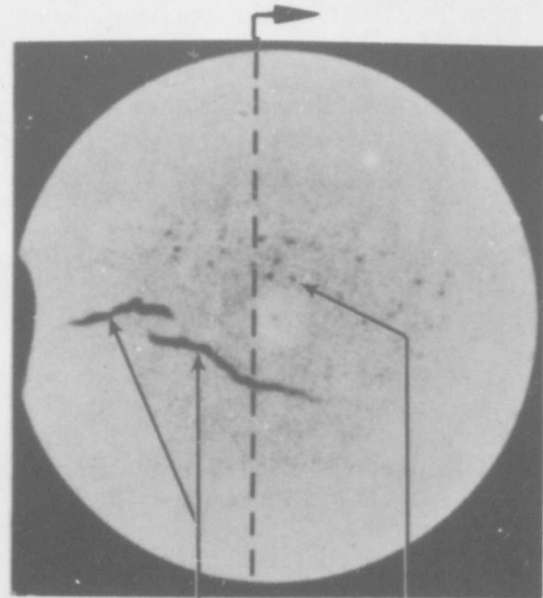
(a) Full Scale Part



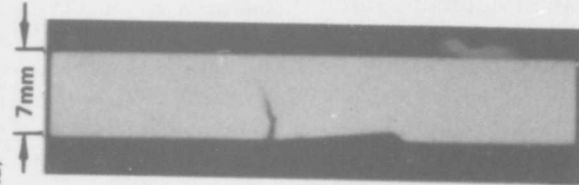
(b) Excised Coupon (42 mm dia)



(c) Film X-Ray



(d) CT Scan Near Surface



(e) CT Scan

Figure 3.1-9 PID #120, 0.5 mm surface cracks

### 3.2 Full-Scale Parts

While demonstrating the ability to observe casting defects in small coupons is a first step for assessing CT potential, it is essential that CT be able to detect defects in full-scale castings. Two full-sized castings were selected for preliminary evaluation. The two candidates chosen contained only minor flaws; however, they were fitted with the flawed coupons described in Section 3.1 by inserting them into machined surface holes. The full-scale castings were then scanned as though the flaw was naturally occurring in that location.

The first casting is an aluminum air inlet duct, PID #127. The casting measures 170 x 90 x 90 mm (6.7 x 3.5 x 3.5 inches), and is pictured in Figure 3.2-1(a). A circular hole large enough to accommodate the flaw coupons was machined in the circular flat surface to a depth of about 25 mm (1 inch). The inlet duct contains a large gas pocket flaw that can be seen to the left side of the flat, circular surface in the photograph. No other flaws were detected. The second host casting is a handle-box casting, PID #102, shown in Figure 3.2-1(b). This aluminum casting (340 x 220 x 70 mm (13.4 x 8.7 x 2.8 inches)) contains minor shrinkage in one surface.

The shrinkage holes (PID #118A) and the crack (PID #120) test coupons were used as the "defect inserts" in the full-scale host castings. The defects were detected with CT but with less detail than when the coupons were scanned separately.

#### 3.2.1 Inlet Duct Casting, PID #127

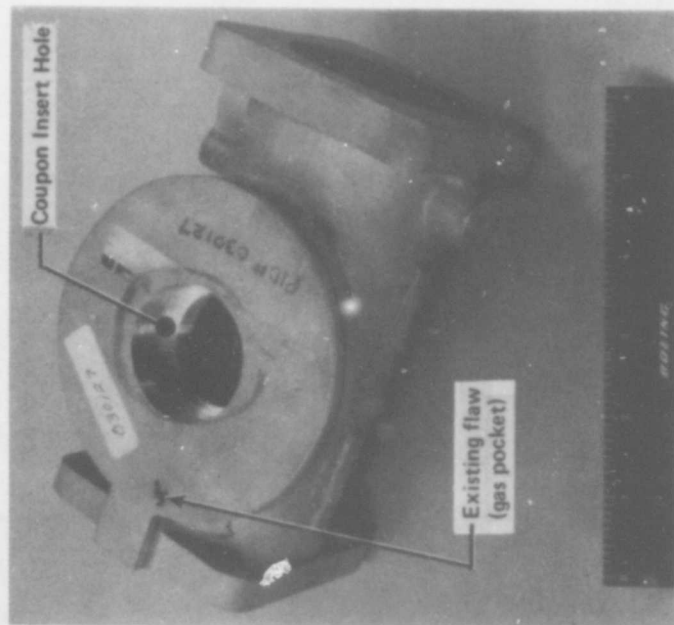
The inlet duct was scanned on Systems B and L. Figures 3.2-2(a) and (b) show a comparison of images of PID #118A scanned alone and scanned while inserted in the larger inlet duct host casting, respectively, on System L at 350 kV. There is a loss in shrinkage flaw definition due primarily to the additional noise evident in Figure 3.2-2(b). The signal-to-noise ratios are 175 and 51 for the test coupon alone and inserted in the inlet duct, respectively. Figures 3.2-2(c) and (d) are CT scans from System B at 420 kV. The slice planes in Figures 3.2-2(c) and (d) are not necessarily at the same level in the part. The signal-to-noise ratio in the images are 7 and 5, respectively, for the coupon alone and inserted in the inlet duct casting.

Figure 3.2-3 shows the comparison of images of the crack coupon (PID #120) scanned alone and scanned inserted in the inlet duct casting, on System B at 225 kV. The crack is less distinct but readily detected when it is inserted in the larger casting structure. The signal-to-noise ratios are 19 and 2.5 for the coupon alone and inserted in the inlet duct, respectively. Again, the slice planes are not necessarily at the same level in the part.

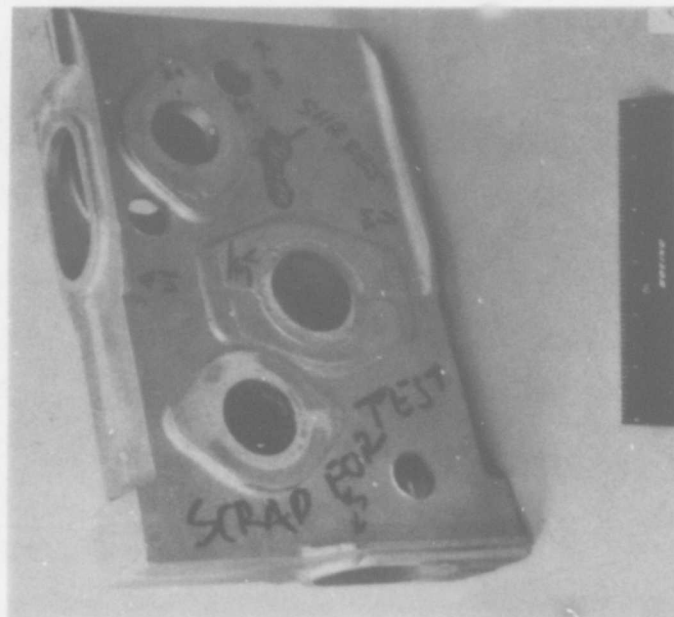
#### 3.2.2 Handle-Box Casting, PID #102

The handle-box casting is larger than the inlet duct, and was CT inspected on System I which has a 2 MV source and a large field of view. Figures 3.2-4(a) and (b) are scans of test coupons PID #120 and PID #118A, respectively. Figure 3.2-4(c) shows the CT slice of the handle box with both of the test coupons inserted. The cracks and porosities in the test coupons were detectable when scanned in the full-scale casting. Figure 3.2-4(d) shows an enlargement of the PID #118A coupon region. There is an obvious reduction in the definition of the defect indications in this image of PID #118A as when compared to Figure 3.2-4(b). Note that (d) is reversed from (b), also the slice planes may not be exactly the same. In Figure 3.2-4(b) holes of approximately 6 x 3 mm (0.24 x 0.12 inch), 2 x 3 mm (0.079 x 0.12 inch), and 1 mm (0.039 inch) across are labelled 1, 2, and 3, respectively, and are easily detected. In Figure 3.2-4(d) holes 1 and 2 are easily detected and even 3 is detectable.





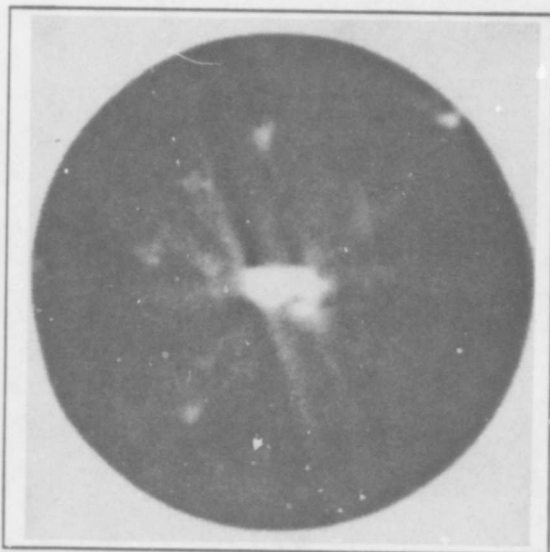
(a) PID # 127, Air Inlet



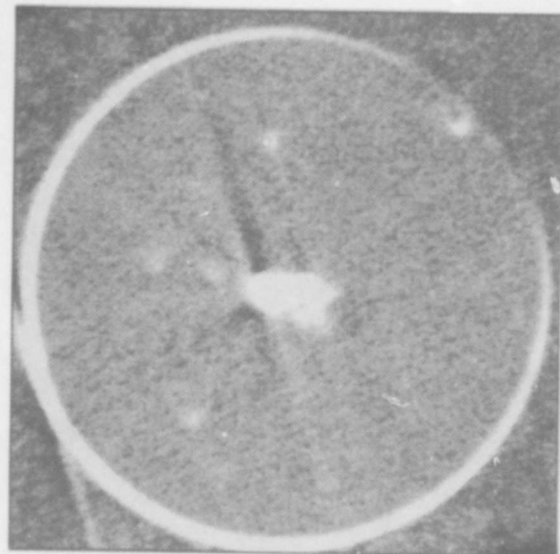
(b) PID # 102, Handle Box

Figure 3.2-1 Full-scale castings

System L

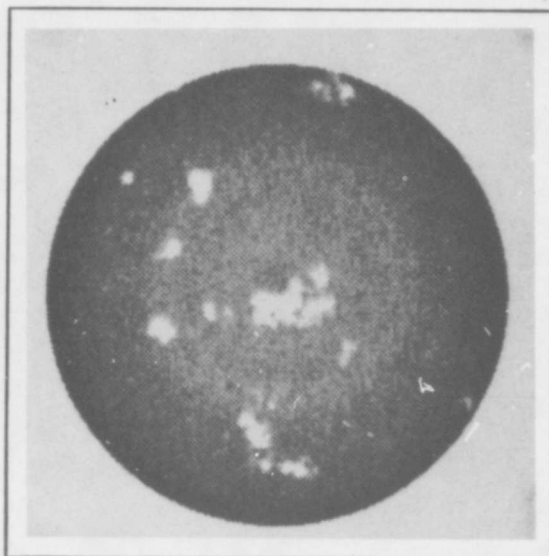


(a) Alone

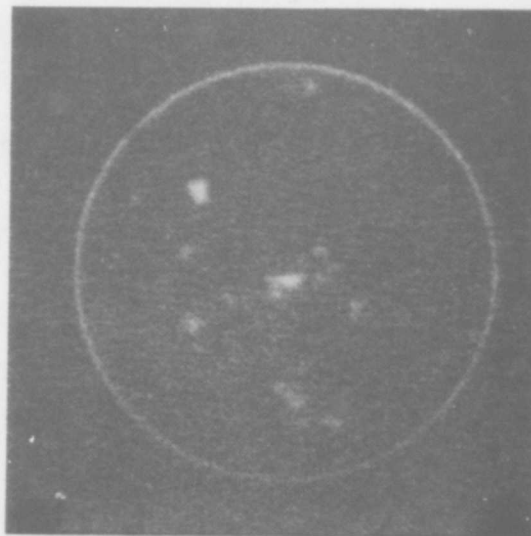


(b) Inserted Into PID # 127

System B



(c) Alone



(d) Inserted Into PID # 127

Figure 3.2-2 CT scans of PID #118A, alone and inserted in Inlet duct casting, showing shrinkage holes



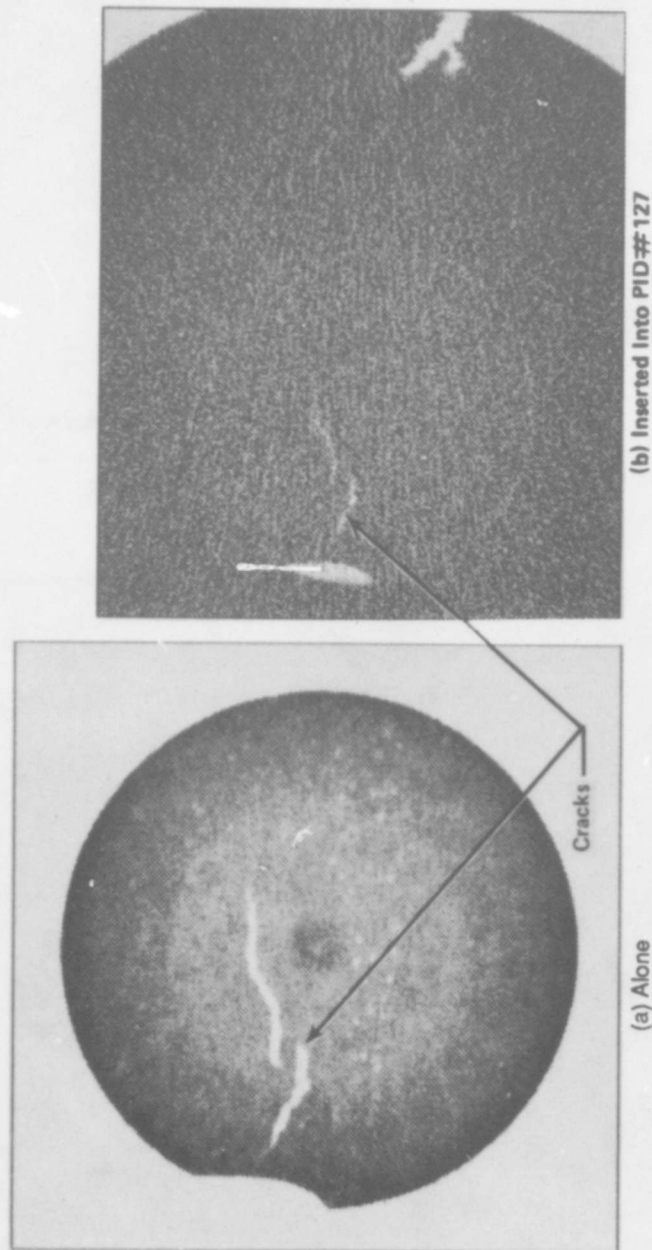
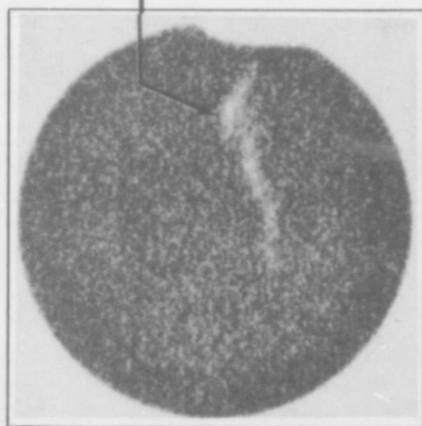
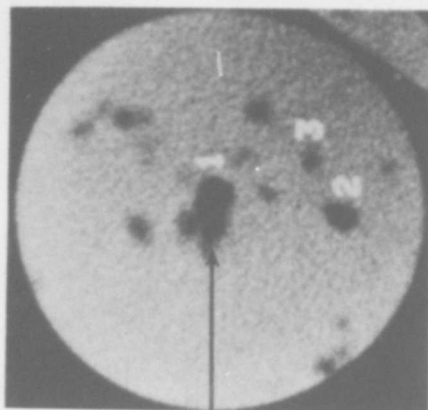


Figure 3.2-3 CT scans of PID #120 alone and inserted in Inlet duct casting



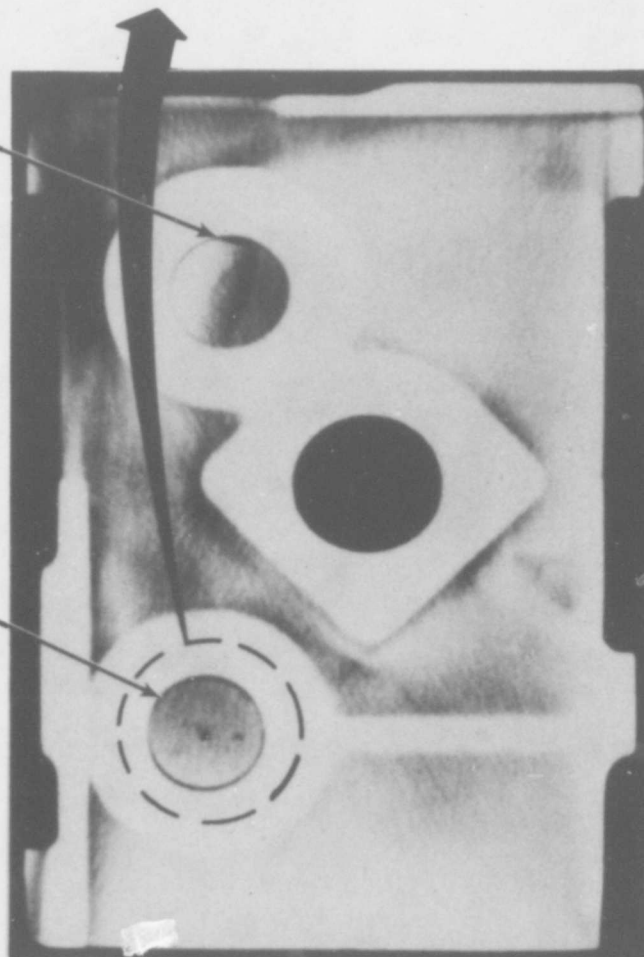
(a) PID #120 Crack Alone (4-mm Slice Width)



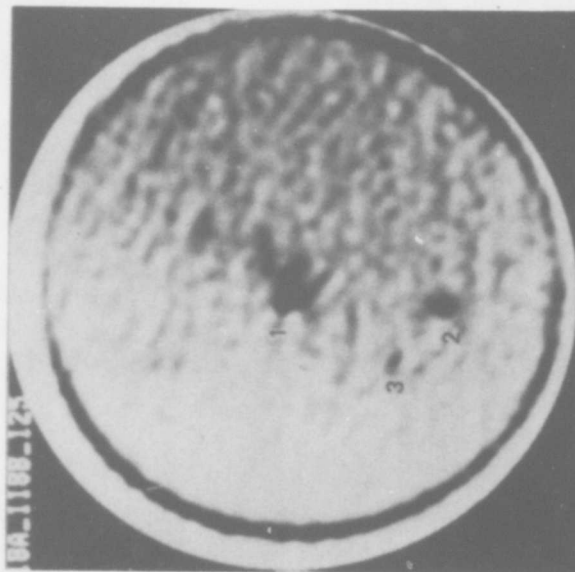
(b) PID #118A Alone (2-mm Slice Width)

Crack (PID #120)

PID #118A



(c) 3-mm Slice Width of PID #120 and 118A Inserted Into PID #102



(d) PID #118A Inserted

Figure 3.2-4 PID #118A and #120 Inserted In handle-box casting

### 3.3 Dimensional Measurements

Dimensional measurements of finished parts are very important in casting manufacture. Two specially machined samples were made for preliminary evaluation of CT dimensional measurements capability. The dimensional phantoms are described in Appendix C. The small (40 mm (1.57 inch) diameter x 25 mm (1 inch)) aluminum phantom contains five accurately machined gaps (3, 1, 0.5, 0.25, 0.125 mm (0.12, 0.04, 0.02, 0.01, 0.005 inch)) and three holes (3, 1, 0.5 mm (0.12, 0.04, 0.02 inch) diameter). This phantom is used to determine small gap measurement accuracy from CT. The larger (380 mm (15 inch) diameter) stainless steel phantom simulates high-alloy cast jet engine components for wall thinning measurement by varying the thickness of two spokes using steps of 0.25 mm: (0.01 inch) and 0.12 mm (0.005 inch).

#### 3.3.1 Aluminum Dimension Phantom, PID #000801

Dimensional measurement of the machined gaps in the small aluminum phantom were made from CT images obtained on four different CT systems. Figure 3.3-1 shows a CT scan image of the phantom from System J. The test phantom was scanned both alone and inserted in the inlet duct (PID #127) on two of the systems. The measurement results for each CT image are shown in Figure 3.3-2. The results indicate that accurate and precise measurements, better than 50 microns (0.002 inch), are possible in the high contrast large gap regions. The values are well within the accuracy range for common casting tolerances of 0.50 to 0.75 mm (0.020 to 0.030 inch) and even precision castings with tolerances down to 0.05 mm (0.002 inch). The results are in agreement with other reports on dimensional accuracies and precision of measurement from CT [3,4]. The accuracy does decrease as the gaps narrow because the image contrast (modulation) is reduced. Also, the precision is reduced when the phantom is inserted in a larger component, apparently due to noise.

The dimensional measurements were obtained by using line plots across the gaps and measuring the gap size at a preset CT value level on the trace. Figure 3.3-3 shows plots across each gap for System J. The CT level used for measuring the gap width was the 50 percent CT value between the air and aluminum CT values in the image. This approach provides an accurate measurement when the gap is large (e.g., 3 mm (0.12 inches)). In the case of the 3 mm (0.12 inch) gap, the contrast level across the gap is high, and the measurement accuracy is representative of measurements across any region (exterior or interior) of a part where a large contrast edge is present. As the gap narrows, the contrast level between the aluminum and the air in the gap is reduced. For the 0.125 mm (0.005 inch) gap this approach is not feasible because the line trace CT values do not even reach the 50 percent CT value.

Figure 3.3-4 shows a plot of the CT level setting (labelled crossover percentage to represent the CT value as a percent of the full modulation between air and metal) which would give the correct measurement of the gap for Systems L and J as a function of gap width. In the case of System L the crossover percentage increases more rapidly than for System J as the gap width decreases. This data confirms that the modulation is decreasing more rapidly in System L (a 1 lp/mm system) which has inherently less resolution than System J (a 2 to 4 lp/mm system) as discussed in CT system performance data of Figure 2.2-1.

The Figure 3.3-1 data shows that when the dimensional phantom was inserted in the inlet duct (PID #127), the measurement precision was reduced. The standard deviation of the gap measurements increased significantly in several cases. This loss in precision is due primarily to a decrease in the signal to noise in the image when the phantom is inserted in a larger object. For example, the signal-to-noise ratios for the phantom images from System B were 32 with the phantom alone and 6 with the phantom inserted.

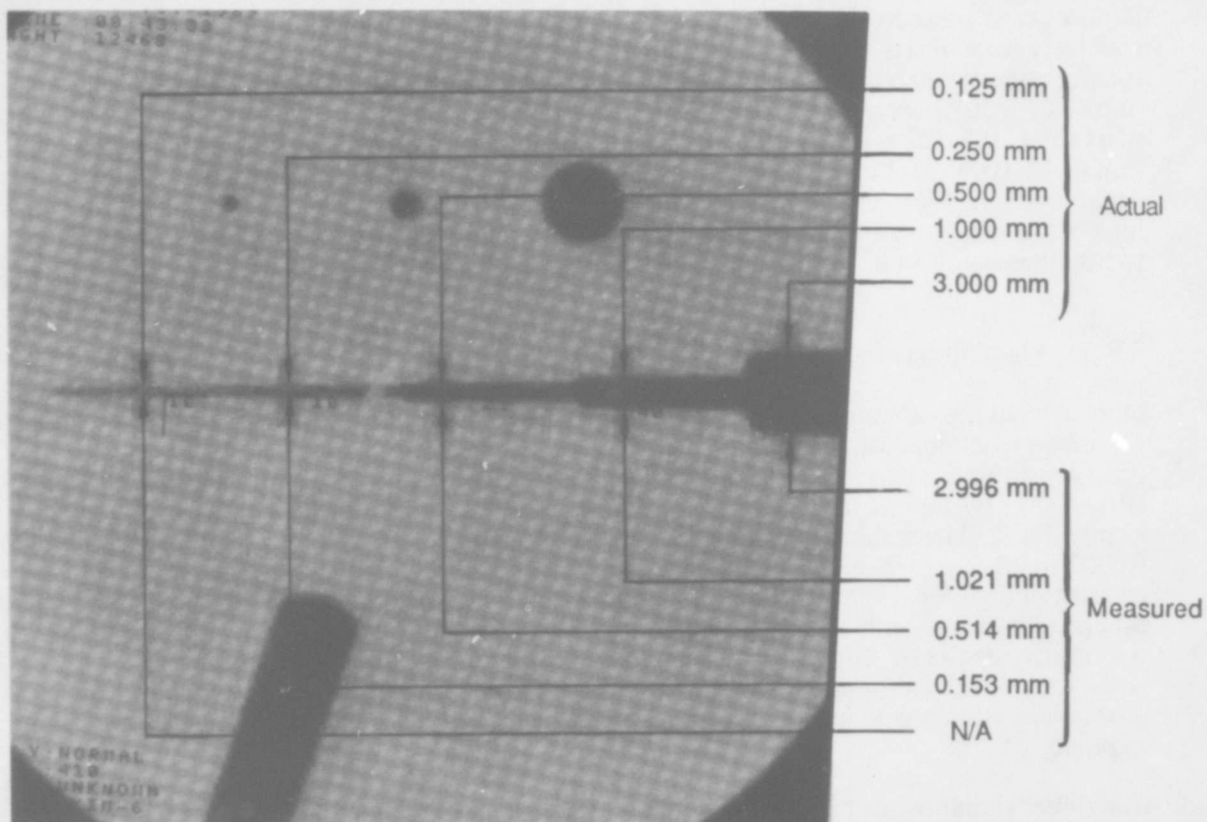


Figure 3.3-1 Aluminum dimensional phantom CT scan from System J

Measured Gap Width

Actual Gap Width (mm)	System B		System L		System J	System I
	Alone	Inserted	Alone	Inserted	Alone	Alone
3.000	$2.992 \pm 0.019$	$3.084 \pm 0.053$	$2.953 \pm 0.015$	$2.982 \pm 0.021$	$2.996 \pm 0.013$	$3.010 \pm 0.054$
1.000	$1.098 \pm 0.021$	$1.158 \pm 0.104$	$0.987 \pm 0.004$	$0.956 \pm 0.045$	$1.021 \pm 0.008$	$0.972 \pm 0.058$
0.500	$0.616 \pm 0.017$	$0.649 \pm 0.162$	$0.217 \pm 0.018$	$0.040 \pm 0.037$	$0.514 \pm 0.009$	
0.250	$0.311 \pm 0.021$	$0.157 \pm 0.106$			$0.153 \pm 0.029$	
0.125						

Figure 3.3-2 Results of dimensional measurements

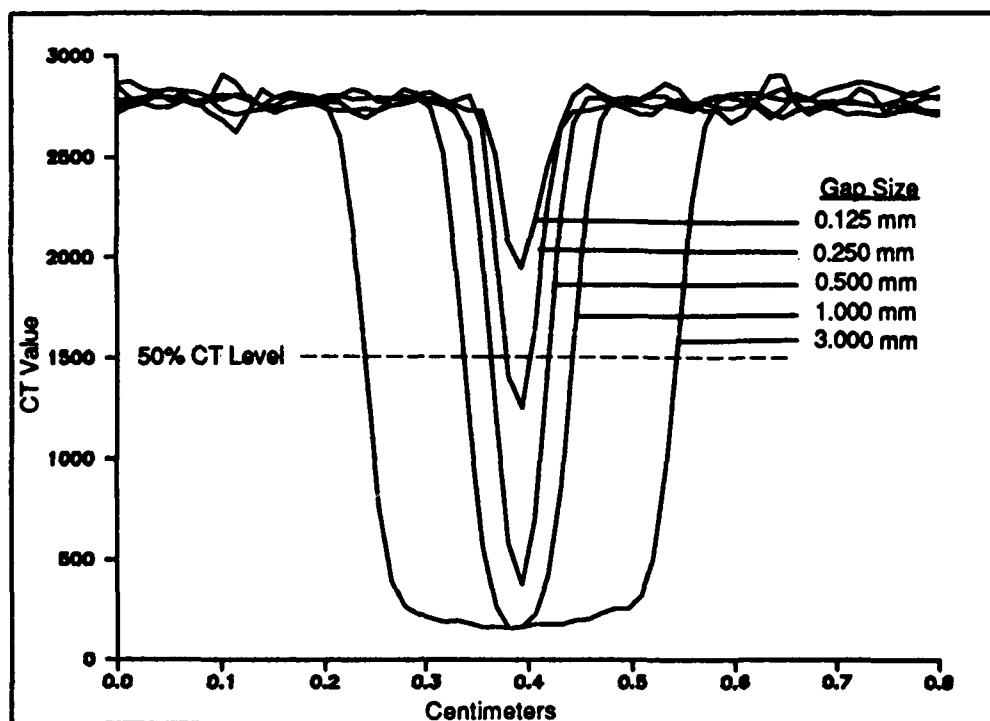


Figure 3.3-3 Line plot traces across aluminum dimensional phantom gaps, System J

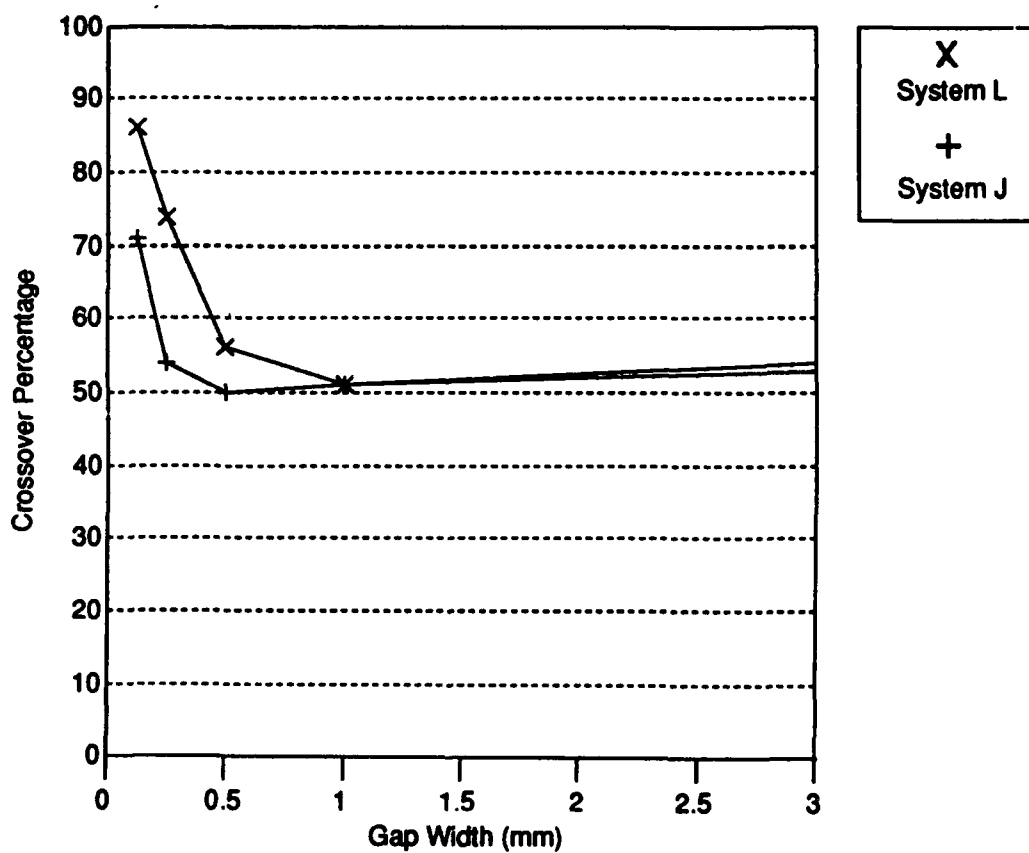


Figure 3.3-4 Crossover percentage vs gap width

### 3.3.2 Steel Dimension Phantom, PID #000701

The large (380 mm (15 inch) diameter) stainless steel dimension phantom was scanned on a CT system with a 2 MV source capable of penetrating the thickness of steel in this part. Figure 3.3-5(a) is an image from System I. According to the CT performance data listed in Figure 2.2-2, the capability of System I for resolution is at best a few percent at 1 lp/mm; however, the 0.25 mm (0.01 inch) steps can be observed visually on the CT image. The plot in Figure 3.3-5(b), showing the steps, was obtained by summing CT numbers for data traces across the spokes for each image pixel column along the spokes. Figure 3.3-5(c) shows how the data was taken across the spoke. The summation of CT numbers across location B would be larger than across location A because more steel is present. In the plot of Figure 3.3-5(b), the summation is performed at each pixel column in the image. This is a very interesting approach to analyzing data for dimensional accuracy, and it clearly indicates the steps. By calibrating on a standard, this approach could be used to establish acceptance criteria for cast parts dimensional measurements. The accuracy appears to be in the range of 0.125 mm (0.005 inch).

### 3.4 Three Dimensional Results

Volumetric data sets can be obtained by taking contiguous CT slices along the axis of the casting that is being inspected. Data sets of this type have been created for PID #119 (shrinkage), PID #118A (holes), PID #120 (crack) and PID #502 (pipe coupler). Display of these images on a three-dimensional (3D) imaging system is useful for visualizing and understanding defect features. The 3D images shown in this report were created on a PIXAR image processing system.

Figure 3.4-1 is a 3D image of PID #119. The data was obtained from 200 slices taken at 410 kV with 0.125 mm (0.005 inch) slice thickness on System J. Figure 3.4-2 is a 3D image of the casting holes, PID #118A. The data was taken at 350 kV with 1.5 mm (0.06 inch) slice thickness and 1 mm (0.04 inch) slice indexing on System L. Figure 3.4-3 is a 3D image of the crack, PID #120. The data was obtained from 60 slices taken at 410 kV with 0.125 mm (0.005 inch) slice thickness on System J. Figure 3.4-4 shows a steel pipe coupler, PID #502, that was scanned on System I with 22 slices and 3 mm (0.12 inch) slice spacing. The aspect ratio of this part is slightly distorted in the display.

The reproduction of the three-dimensional images in this report does not do them justice as compared to the visualization possible when observing the data on the image processing system directly. The PIXAR image processing system can present the data in motion so that the observer can visualize how the defects are oriented in the part geometry. The images are created by windowing a region of CT numbers which include the flaws from the image data set. The edge of the part will have a level at which the CT number falls into the window and therefore the part edges will be defined. Transparency in the display of features allows the inspector to see through the wall and observe internal details. A video tape of the three-dimensional studies showing the objects in motion has been produced.

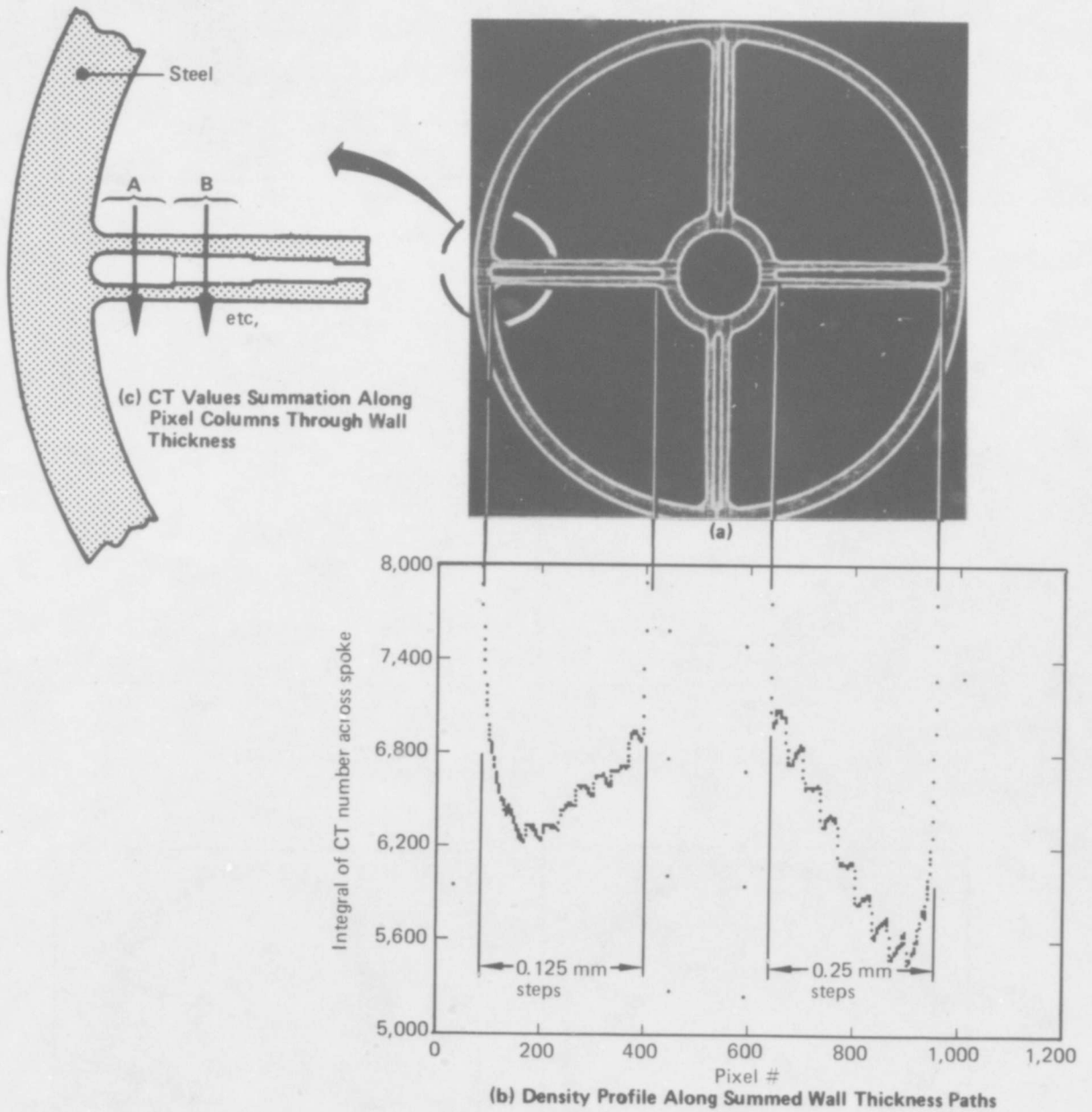
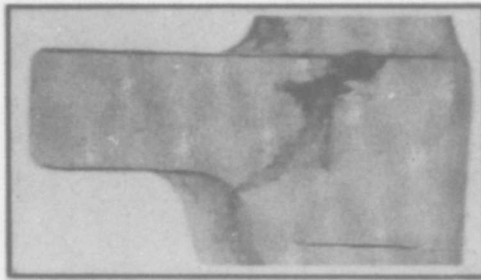
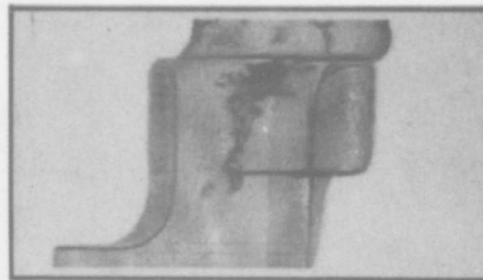


Figure 3.3-5 Steel dimensional phantom results



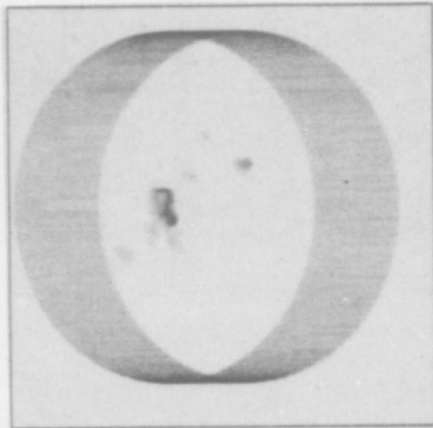


(a)

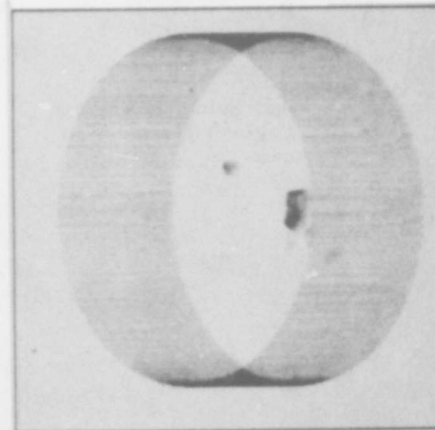


(b) Rotated 240°

Figure 3.4-1 Two selected 3D views of PID #119 (shrinkage)

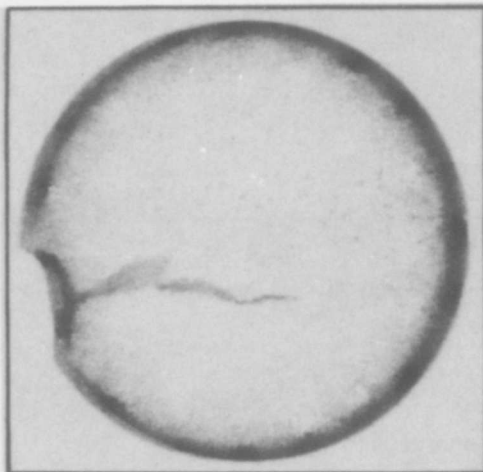


(a)



(b) Rotated 180°

Figure 3.4-2 Two selected 3D views of PID #118A (holes)



(a)



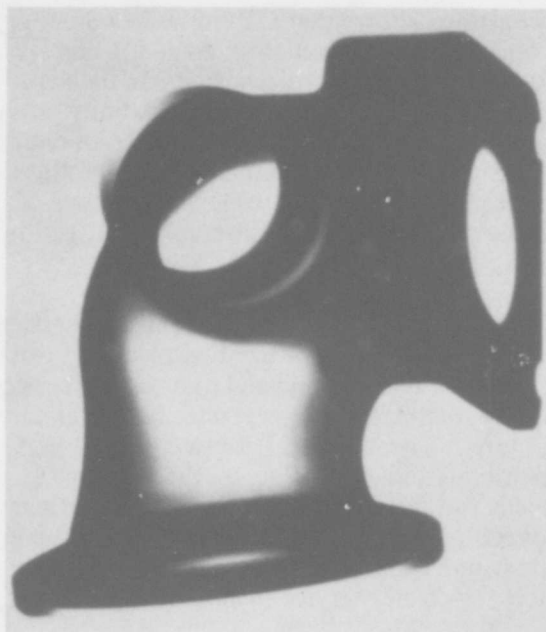
(b) Rotated 210°

Figure 3.4-3 Two selected 3D views of PID #120 (crack)

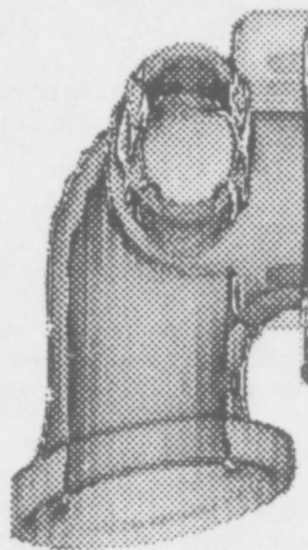




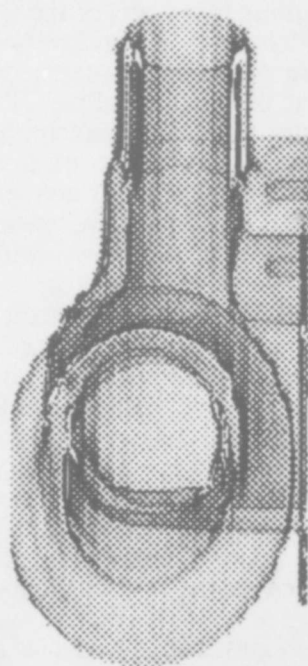
(a) Photo of PID #502



(b) Film X-ray of PID #502



(c) 3D view 1 of PID #502



(d) 3D view 2 of PID #502, rotated 60°

Figure 3.4-4 PID #502, steel elbow casting

## 4.0 COST BENEFIT ANALYSIS

The preliminary results of the CT examination of castings shows that CT can detect a variety of casting defects to various levels depending on the object size and geometry. Also, CT can provide dimensional measurement capability with accuracies better than 50 microns (0.002 inches). The economic incentive to utilize CT on castings is dependent upon the benefits this capability provides to industry. Casting manufacturing engineers estimate, for aerospace castings, that from one-third to two-thirds of the cost of a casting is the current inspection requirements and practices. In addition, present nondestructive evaluation techniques are limited with respect to the type of data they produce and the completeness of the data. Visual, penetrant and radiographic inspection are the techniques required by specification such as MIL-STD-2175.

Castings represent an important component in the aircraft/aerospace industry, but presently they make up only a few percent of the weight of an aircraft and are not used as primary structure except in a few instances. Provided sufficient inspection capability existed to establish structural damage tolerance, castings could replace more costly manufacturing practice, be designed with reduced weight and be utilized as primary structure. The potential for weight savings, for example, is in the range of \$200/lb for commercial aircraft and, depending on the mission, \$500/lb and higher for military aircraft. Even a few percent weight savings can become significant on fleets of hundreds of aircraft. Combined with reduced manufacturing cost of 100 to 500 percent for castings over alternatives, there is keen interest in manufacturing engineering to establish acceptance criteria that would make castings available for greater service in aircraft applications.

Three categories of potential for applying CT to castings and achieving economic return are: 1) On-line inspection, 2) Performance engineering evaluation, and 3) New product development/first article inspection.

### 4.1 On-line Inspection of Castings

Castings manufactured for aircraft/aerospace applications will often have stringent inspection requirements. For large investment castings used in turbine engines the requirement will include 100 percent radiographic inspection. The written procedure may consist of over 200 pages and require more than 1000 radiographic exposures. This level of inspection can add over \$30,000 to the cost of a component. One hundred percent CT inspection of even large (1500 mm (59.1 inch) diameter) cast structures is possible with CT at relatively economical costs. However, the level of detail sensitivity, relative to film radiography, with existing CT machines for large castings is not yet established.

The costs of CT scanning can vary significantly based on the type of system and size of part. Typical costs experienced to date on this program range from approximately \$2.5 to \$10 per slice for medical CT systems to approximately \$20 to \$60 per slice for industrial CT systems. For 100 percent inspection it is not uncommon to expect 100 to 300 slices to be used. It was shown in the study of the filamentary shrinkage, PID #119, that moving to a medical CT system could still detect defects, but not define them. In this example, a much faster and less expensive CT inspection is used and, if the detection sensitivity is sufficient, a very cost effective approach is possible.

Current inspection of castings can encounter difficulty with interpretation. On one aircraft casting example, with a part value of several hundred dollars, the nearly 3000 parts produced since 1962 had successfully passed inspection. When the inspection responsibility (interpreters) was changed, with no change in manufacture or inspection procedure, the new interpretation of results caused 100 percent rejection and several hundreds of thousands of dollars in additional costs. This example is not unique and is symptomatic of casting inspection. The interpretation of results can

be highly subjective. Also, there appears to be no definable or predictable correlation between the data and the casting performance. None of the approximately 3000 parts in service had ever failed. CT is capable of providing a more quantitative and less subjective inspection method than current techniques.

For economic use of CT as an alternative to current inspections, the cost must be competitive with the present inspection cost. While inspection costs for castings vary widely depending on the part and its mission, it is expected that total CT inspection costs need to fall into the range of \$20 to \$100 per part to be competitive on average aerospace castings. One issue of concern is the real need for 100 percent CT inspection. RT for example is not a truly 100 percent inspection. Although the film coverage may be over an entire part, the sensitivity to detail is certainly not the same over that coverage because of the complex shape of castings. The percentage of inspection on a casting at specified sensitivity varies widely, but on average could be less than 20 percent of the part. Thus, equivalently, CT coverage of only 20 percent would be sufficient. A real advantage of CT is that coverage could be specified for only critical areas. An even better approach is a combination of DR and CT that can be very cost effective and can provide high confidence inspection. In this approach a DR is taken over the entire part and CT slices are taken at questionable locations from the DR interpretation or at preassigned critical points. Throughput from this approach can be quite high. This is the approach successfully used for turbine blade inspection.

#### 4.2 Performance Engineering Evaluation

No other single factor restricts the wider general use of castings in aircraft/aerospace applications more than the inability to determine, with a high degree of accuracy, how the castings will perform in service. Unlike wrought, forged or extruded metal products, castings lack the properties so essential for predictability of long-term performance. Because castings are complex structures, exhibiting a large indeterminate range of properties and structural characteristics, they have never been thoroughly evaluated with respect to their tolerance for all the various deficiencies of structure and properties for which they are routinely inspected. In addition to this very fundamental problem, there exists an even more serious shortcoming in the manner in which castings are presently inspected and judged to be acceptable or not. That is, there are no casting inspection criteria in use in the aerospace industry today that are quantitatively related to a predictable loss of casting properties. If an effective casting inspection system can be developed utilizing computed tomography to provide accurate flaw size and spatial location data necessary for structural damage tolerance analysis, aerospace manufacturing engineers estimate that casting utilization would double or triple over present levels and casting costs would decline to perhaps one-half to one-third of today's price in the aerospace industry.

Because the present casting inspection methods cannot provide quantitative information, design and structural engineers are understandably reluctant to take anything other than an extremely conservative approach to the wider use of castings in aerospace applications. There is a real possibility that over-design, resulting from the imposition of the typical 1.33 casting factor, makes all but the most superficial visual inspection for major external flaws unnecessary. Significant savings in aircraft/aerospace applications could result from suitable inspection technology that could eliminate the need for the 1.33 casting factor, allow more castings to be used as primary structure and allow casting designs better suited to the intended service requirements.

A structural damage tolerance/computed tomography based casting inspection approach would require the development of the following capabilities: 1) CAD casting design, 2) Finite element analysis and problematic failure analysis, 3) Critical flaw size prediction for failure points, 4) Load test confirmation of failure modes and locations, and 5) Input of critical flaw size and location to a CT casting inspection system. This concept is not very far from reality. Progress is being made in

these areas, particularly 1, 2 and 5. As the potential of this concept is communicated to industry, interest will be generated in obtaining the data for areas 3 and 4.

#### 4.3 New Product Development/First Article Inspection

The development of a new cast product follows a considerable process from concept to production. If the casting is aluminum, it will almost invariably be specified to conform to the requirements of MIL-A-21180 and the inspection requirements of MIL-STD-2175. The development process will include: 1) Preliminary design requirements, configuration concepts and cost trade-off studies for all viable production methods (casting, forging, weldment, machined, non-metal, etc.); 2) Two or more production concepts will go to structural analysis and costing by vendor sources; 3) Modification of design to optimize producibility, correct deficiencies and reduce cost; and 4) Source evaluation and selection including NDE techniques. For the actual casting development, the design will be converted to a fabrication practice and test castings made. These will be extensively nondestructively and destructively inspected to establish the optimum method of casting manufacture to avoid defects. CT can play an important role in reducing the cycle time in developing new castings by providing three-dimensional flaw information. This type of data is valuable to casting engineers for understanding the metal flow and solidification behavior so that positioning of sprues and chills can be optimized and defects minimized.

A major cost driver in castings will be the requirement of meeting MIL-A-21180 and MIL-STD-2175. A foundry will typically quote a price three to four times higher than the same casting ordered to commercial standards. Industry experience with these and similar specifications has established that they will require extensive inspection and the results are very high scrap loss rates. Despite the belief that the specifications assure premium quality castings, they are "premium" in the sense that they are relatively flaw free. The "premium" quality that is desired is that the parts have no critical size flaw in locations where in-service stress levels can cause them to grow and propagate in a manner that the casting can no longer perform its intended function. As pointed out in Section 4.2, CT offers the potential for providing this type of inspection data.

On large, critical aircraft/aerospace castings, the first casting articles fabricated must undergo stringent nondestructive and destructive measurements to assure that the casting conforms to the design. Such measurement can result in the destruction of one or more castings worth tens of thousands of dollars and require significant investments in inspection efforts worth several times the casting value. CT has potential to reduce these costs significantly if the dimensional measurement accuracy and defect sensitivity is sufficient for the size of casting.

These benefits of CT for dimensional and flaw distribution measurements of castings are being realized in other industries. For example, the automobile industry in both the U.S. and Japan are employing CT systems for studying castings. The primary emphasis has been in dimensional measurements and product development. Accurate economic factors are not available, but the increasing interest and acquisition of CT systems indicates a positive ROI in a highly competitive market.

#### 4.4 Standards

The economic implementation of CT for castings will not only require that CT show demonstrated inspection capability, but suitable standards and specifications will be required. Although this preliminary task assignment has discussed CT inspection relative to radiographic casting specifications, it should be clear that CT provides a different perspective on defects and present radiographic reference standards are not suitable. The development of new standards and specifications for casting inspection utilizing CT is no small task. However, the overall approach

to CT inspection for damage tolerance/fitness-for-service evaluation is much more desirable than current practice. As such, the economic incentive to move to CT based inspection will exist, provided CT inspection costs are within a comparable range to existing techniques.

## 5.0 CONCLUSIONS AND RECOMMENDATIONS

### 5.1 CT of Castings Conclusions

This preliminary task assignment on CT for castings has identified a number of important issues affecting the potential for economic payoff by using CT on castings. The primary conclusion drawn from the effort is that CT can be more sensitive to flaws than radiography and spatially defines the flaw distribution in depth. By comparing CT sensitivity on small flawed coupons to RT it was observed that CT could readily detect defects in a much more understandable manner than RT. While the RT image contained an integration of flaws throughout the part depth, CT showed where significant flaws existed within the depth of the part and where they did not. This points out that the ASTM classification methodology is not very appropriate for CT because it is an integrated defect criteria and CT can image even very small flaws individually, locating them accurately in the object.

Dimensional measurements from CT data were found to have accuracies better than 50 microns (0.002 inches). The ability to obtain measurements on casting configurations is a significant capability of CT. The measurement accuracy is dependent on the CT system resolution, the image noise and the method of edge detection measurement. The edge detection technique is a topic for further investigation, but it should be possible to increase measurement accuracies by implementing more sophisticated edge detection algorithms. Dimensional measurements of castings is a critical enabling capability for casting development and first article inspection with a high potential for significant cost benefit. In fact, this utilization of CT has been used in the automotive industry in the U.S. and Japan to justify the acquisition of CT systems.

The casting size and geometry were found to affect the CT sensitivity. As the casting size increased, the CT systems were less sensitive to the defects. This is to be expected, and represents a design challenge of matching CT performance to part size and geometry. This problem will require additional study to quantify the various tradeoff effects such as CT system handling size, resolution, and scan time. Artifacts due to part geometry, other than beam hardening, were not a significant issue in the study. However, it is known that in complicated castings reconstruction artifacts due to the part features will influence the detectability of defects. This needs to be quantified and will require further study.

The type of CT system employed was shown to affect detail sensitivity. It was found that small defects could be detected with 1 lp/mm resolution CT systems, but not accurately resolved. This issue is important for production inspection because it is possible to design an inspection scheme such that low-cost, high-speed CT can be used where critical size defects must be detected but not necessarily resolved.

Three-dimensional (3D) data sets of castings provided dramatic defect and feature visualization for engineering evaluation of casting problems. The 3D display allows the image of the part to be rotated in space. The material is given a transparency which allows the inspector to look through external surfaces to observe internal detail, allowing part evaluation by less skilled personnel. The next step in this process is to correlate the images with 3D computer aided design packages and 3D model building technology.

Current specified casting inspection procedures do not relate to quantitative damage tolerance criteria, whereas, CT data is quantitative and has significant potential for use in fitness-for-service evaluation of castings. This is a most important conclusion for the long-term aircraft/aerospace application of castings because the potential to utilize engineering based acceptance criteria could reduce casting rejection rates significantly. Developments in this area are expected to have very high economic payback in the future.

The economic potential of having a quantitative NDE method such as CT is significant in terms of overall reduced manufacturing costs and greater application of castings in industry. This is primarily achieved by being able to accept castings whose defects are in non-critical locations. CT and DR data is digital and more readily processed than radiographic film; as such it has potential to offset radiographic film costs, interpretation effort and archiving costs. The ability to image in complex geometries is also of economically competitive value relative to radiography for which complex geometries are difficult if not impossible to evaluate adequately. Nevertheless, the amortized cost of CT inspection equipment and operation will need to be competitive within a reasonable factor to other NDE methods. This will require further study but appears to be feasible with high-throughput CT systems, as evidenced by the turbine blade industry.

## 5.2 Recommendations

We believe that the application of CT to castings has a high potential for significant payoff. Two key areas need to be addressed in order to accurately assess the economics of implementing CT in casting production. The primary area is to understand the effect of full-scale casting geometry on CT defect sensitivity. Both detection and feature dimensional measurements are affected by the CT system required to handle the part size and provide adequate X-ray penetration, and by the artifacts that may occur from part geometry or CT system operations. These effects need to be quantified as best as possible and techniques for reducing their influence must be developed. Specifically, this would include artifact reduction techniques, edge detection algorithms and dimensional measurement algorithms.

The second area requiring investigation is the applicability of utilizing CT data in structural damage tolerance criteria calculations. Development of this would have far reaching consequences for the economic utilization of not only castings but many engineering materials and processes. By converting CT data into a form suitable for finite element modeling, this process can be enabled. The driving issue is to ultimately develop inspection acceptance criteria on cast parts that is matched to how they will perform in service.

In addition to these key areas, further experimentation on high-throughput CT equipment is needed. This effort is necessary to accurately establish the economic factors for CT systems as they may be applied to castings. The progress being made in CT system capabilities are resulting in reduced CT inspection costs for castings.

## **6.0 REFERENCES**

1. R. H. Bossi, R. J. Kruse, B. W. Knutson, "X-Ray Computed Tomography of Electronics", WRDC-TR-89-4112
2. R. H. Bossi, J. L. Cline, B. W. Knutson, "X-Ray Computed Tomography of Closed Systems", WRDC-TR-89-4113
3. H. Ellinger, Suzanne Buchele and Forrest Hopkins, "Dimensional Analysis of Foundry Castings using Computerized Tomography", Proceedings of American Foundry Society, St. Louis, MO, 1987
4. "Standard Guide for Computed Tomography (CT) Imaging", ASTM, 1990, to be released



## APPENDIX A X-RAY IMAGING TECHNIQUES

The three techniques of X-ray imaging used in the castings task assignment are film radiography, digital radiography, and computed tomography.

### A1 Film Radiography

Conventional film radiography, as illustrated in Figure A1-1, uses a two-dimensional radiographic film to record the attenuation of the X-ray radiation passing through a three-dimensional object. This results in a shadowgraph containing the superposition of all of the object features in the image and often requires a skilled radiographer to interpret.

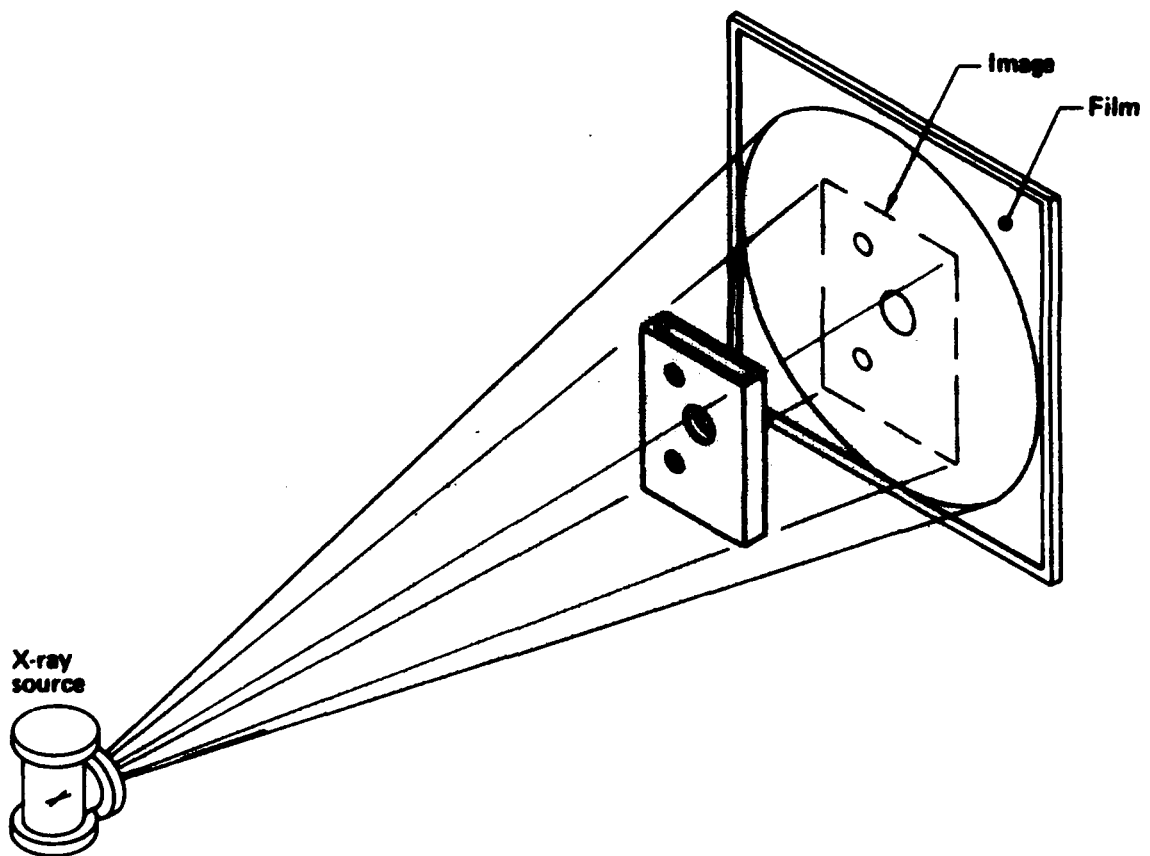


Figure A1-1 Film radiography

## A2 Digital Radiography

Digital radiography (DR) is similar to conventional film radiography. The DR is performed on a system where the film is replaced by a linear array of detectors and the X-ray beam is collimated into a fan beam as shown in Figure A2-1. The object is moved perpendicular to the detector array and the attenuated radiation is digitally sampled by the detectors. The data is 'stacked' up in a computer memory and displayed as an image.

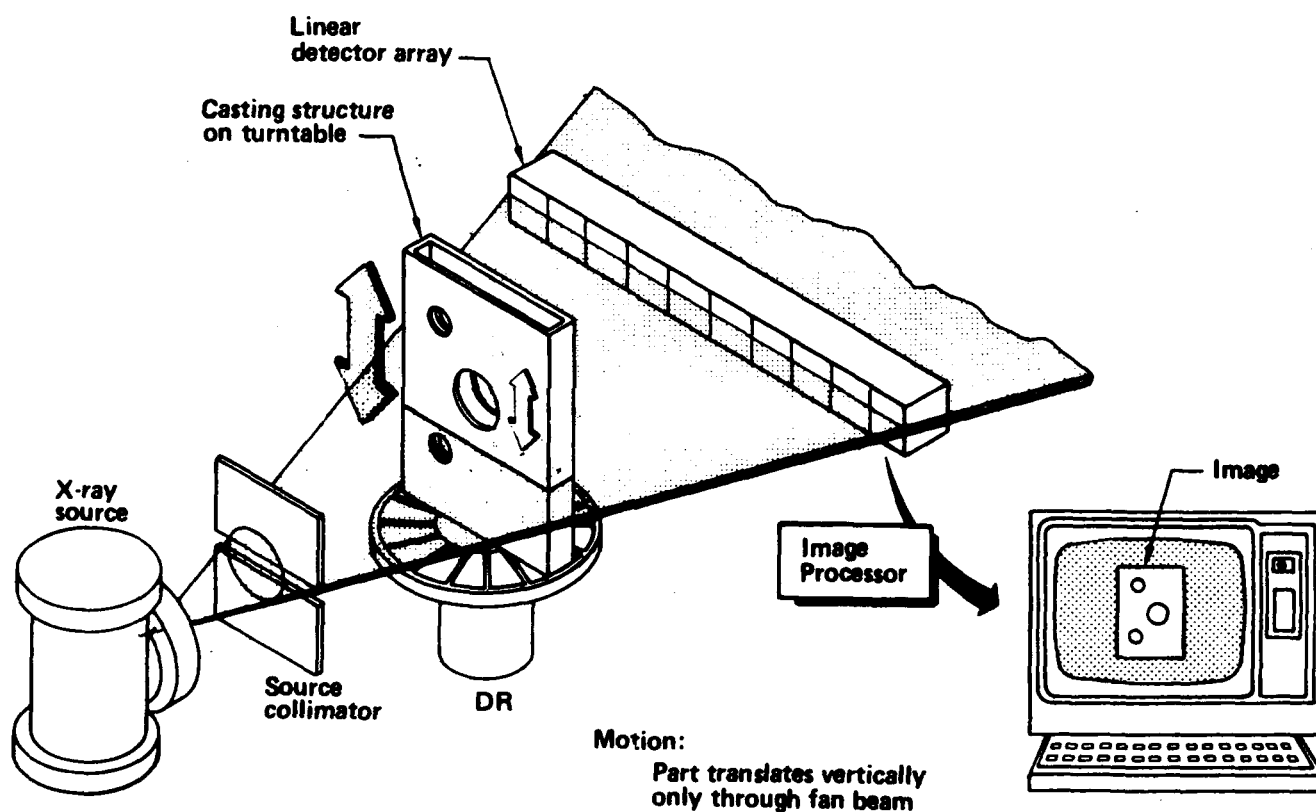


Figure A2-1 Digital radiography

### A3 Computed Tomography

Computed tomography (CT) produces cross-sectional images of thin planes of an object. To generate a CT image, X-ray transmission is measured by an array of detectors as shown in Figure A3-1. Data is taken by translating and rotating the object so that many viewing angles about the object are used. A computer mathematically reconstructs the cross-sectional image from the multiple-view data collected. A primary benefit of CT is that features are not superimposed in the image thus making it easier to interpret.

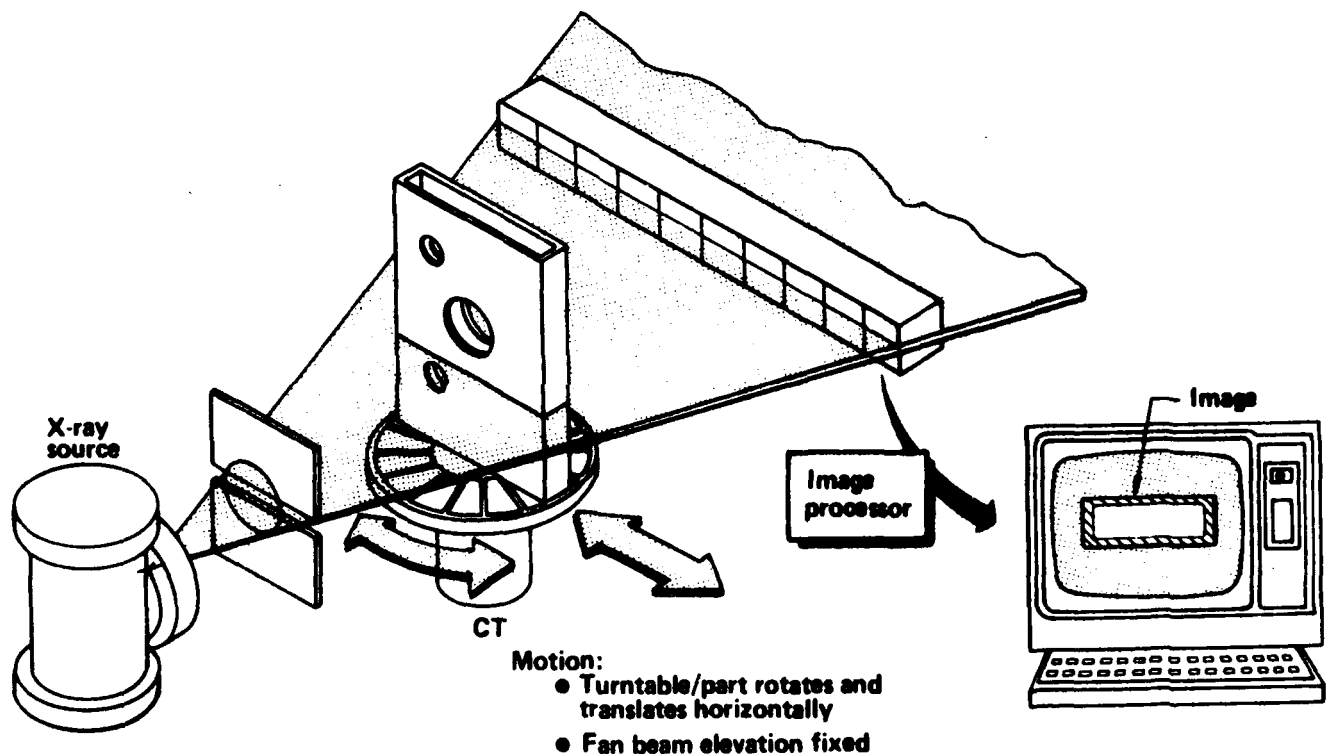


Figure A3-1 Computed tomography

## APPENDIX B FOUNDRY CONTACT LIST

<u>FOUNDRY CONTACTED</u>	<u>TYPE OF FOUNDRY</u>	<u>ALLOYS POURED</u>
Arwood Corporation 3855 West 150th St Cleveland, OH 44111	Investment	Ferrous & Non-Ferrous
Atlas Foundry & Machine Co. 3021 S. Wilkeson St. Tacoma, WA 98409-8857	Sand	Ferrous
Aurora Engineering 1451 E. Main St. Santa Paula, CA 93060	Investment	Aluminum
Beals Casting 520 Suth Palmetto Ontario, CA 91762	Sand	Aluminum
Bralco, Inc. 7620 2nd Ave S. Seattle, WA	Sand	Aluminum & Brass
Cercast, Inc 3905 Industrial Blvd Montreal North Quebec H1H272	Investment	Aluminum
Cercon Casting Corp. 201 Consolidate Dr. Hillsboro, TX 76645	Investment	Aluminum
Coastcast 14831 Maple Ave Cardena, CA 90247	Investment	Ferrous & Non-Ferrous
Fansteel/Wellman Dynamics P.O. Box 147 U.S. Route 34 Creston, IA 50801	Sand	Aluminum & Magnesium.
Golden State Castings 4008 134th N.E. Marysville, WA 98270	Investment	Ferrous & Non-Ferrous
Hemet (AMCAST) Steel Casting Co. 11000 Hersey Blvd Rancho Cucamonga, CA 91730	Investment	Steel

<b><u>FOUNDRY CONTACTED</u></b>	<b><u>TYPE OF FOUNDRY</u></b>	<b><u>ALLOYS POURED</u></b>
Hemet (AMCAST) Casting Co. 760-West Acacia Ave. Hemet, CA 92343-4044	Investment	Aluminum
Hichcock Industries Inc.and 8701 Harriet Ave S. Minn, MN 55420	Sand	Aluminum & Magnesium
Hitchiner Mfg Co. P.O. Box 220 O'Fallon, MD 63366	Investment	Aluminum
Hollywood Alloy Casting Co. 2000 Santa Fe Ave Compton, CA 90220	Sand	Aluminum
Howmet TI-Cast Division 1600 S. Warner St. Whitehall, MI 49461\	Investment	Titanium
Linmold Co. 400 East Carlin Ave Compton, CA 90224	Sand	Aluminum
Lo Nigro Castings 145 Pacific St. Pomona, CA 91768	Sand	Aluminum
Magparts 1545 Roosevelt St. Azusa, CA 91702	Sand	Aluminum & Magnesium
Morel Foundry 3400 26th Ave S.W. Seattle, WA 98106	Sand	Aluminum
PAC Foundries 705 Industrial Ave Port Hueneme,CA 93041	Investment	Ferrous & Non-Ferrous
Precision Castparts Co. 4600 S.E. Harney Dr Portland, OR 97206	Investment	Ferrous  Non-Ferrous
Precision Founders, Inc 414 Hester St. San Leandro, CA 94977	Investment	Ferrous
Presto Casting 5440 W. Missouri P.O. Box 1059 Glendale, AZ 85311	Sand	Magnesium

<u>FOUNDRY CONTACTED</u>	<u>TYPE OF FOUNDRY</u>	<u>ALLOYS POURED</u>
Riverside Foundry 4008 134th N.E. Marysville, WA 98270	Sand	Aluminum
Seacast, Inc. 207 So. Bennet St. Seattle, WA 98108	Sand	Aluminum
Sigma Casting Corp. 1011 Charlie Road City of Industry, CA 91748	Investment	Aluminum
Sunset Foundry Co. 8828 So. 206th St Kent, WA 98035	Sand	Aluminum
Teledyne Cast Prod. 4200 W. Valley Blvd Pomona, CA 91766	Sand	Aluminum
Tiernay 2818 E. Illini Phoenix, Az 85040	Investment	Ferrous & Non-Ferrous
Titech Int, Inc 4000 W. Valley Blvd Pomona, CA 91769	Investment	Titanium
V&W Castings 6032 Shull Street Bell Gardens, CA 90201	Sand	Aluminum

## APPENDIX C CT PHANTOMS

A set of CT phantoms was developed for the Advanced Development of X-ray Computed Tomography Applications program in order to provide consistent evaluation of results from various CT systems. The phantoms serve several purposes. First, they provide a quantitative measure of the CT machine capability that can be used repetitively to assure consistent performance. Second, the quantitative measurements can be used in conjunction with part images to assess a quality level necessary to achieve desired detection or measurement levels in the inspected parts. Third, the phantoms can be used to select CT systems based on the desired sensitivity level for the CT application.

The use of phantoms for CT is complicated due to the wide range of parameters in any CT inspection. Therefore, caution must be used in extrapolating phantom data to suggest a "best" overall CT system. In fact, CT systems have varying designs that result in a range of performance characteristics. The phantoms allow the user a quantitative measure of quality level that, combined with other operating parameters, may suggest an optimum system. While the phantoms used in this program measure line pair resolution and contrast sensitivity, there are several other important parameters a user must be concerned with in selecting a machine for scanning: scan time, field of view, object penetration, data manipulation, system availability and cost.

Three basic CT performance phantoms and two dimension measurement phantoms have been constructed. The CT performance phantoms are: line pair resolution phantom, contrast sensitivity phantom and a density standard phantom. The resolution and contrast sensitivity measurements are fundamental measures of a system. The density measurement is more of a calibration. The dimensional measurement phantoms are of two types, one for general small CT system gap measurements and one for larger CT system wall measurements.

### C1 Resolution Phantom

Figure C1-1 shows the line pair resolution phantom. The phantom consists of sets of metallic and acrylic plates of specified thicknesses. Line pairs of 0.5, 1, 2 and 4 lp/mm are formed by the phantom.

The entire assembly is bolted together and the line pair plates can be changed if additional or a different range of line pairs is desired. Following CT scanning the reconstructed image is analyzed by measuring the modulation of the CT numbers resulting from a trace across the line pairs. The modulation at each line pair set is measured as a percentage of the modulation, where the modulation measured between the 3 mm (0.12 in) thick metal reference bar and 3 mm (0.12 in) thick acrylic steps is 100 percent. Operating parameters such as field of view, slice thickness, integration time and detector collimation will affect the results. It is desirable to obtain data at CT machine parameters that are the same as that used for part scanning. The resolution phantom has been fabricated in two forms, steel/acrylic and aluminum/acrylic. The steel/acrylic phantom is for systems of 300 kVp and up, the aluminum/acrylic phantom is for systems under 300 kVp.

Figure C1-2 shows a CT image of the steel resolution phantom obtained from a high-resolution CT machine. The CT image density contour line across the gauge indicates modulation for the respective line pair measurements at approximately 82 percent at 1/2 lp/mm, 46 percent at 1 lp/mm, 4 percent at 2 lp/mm, and 0 percent at 4 lp/mm.





Figure C1-1 Photo of resolution phantom

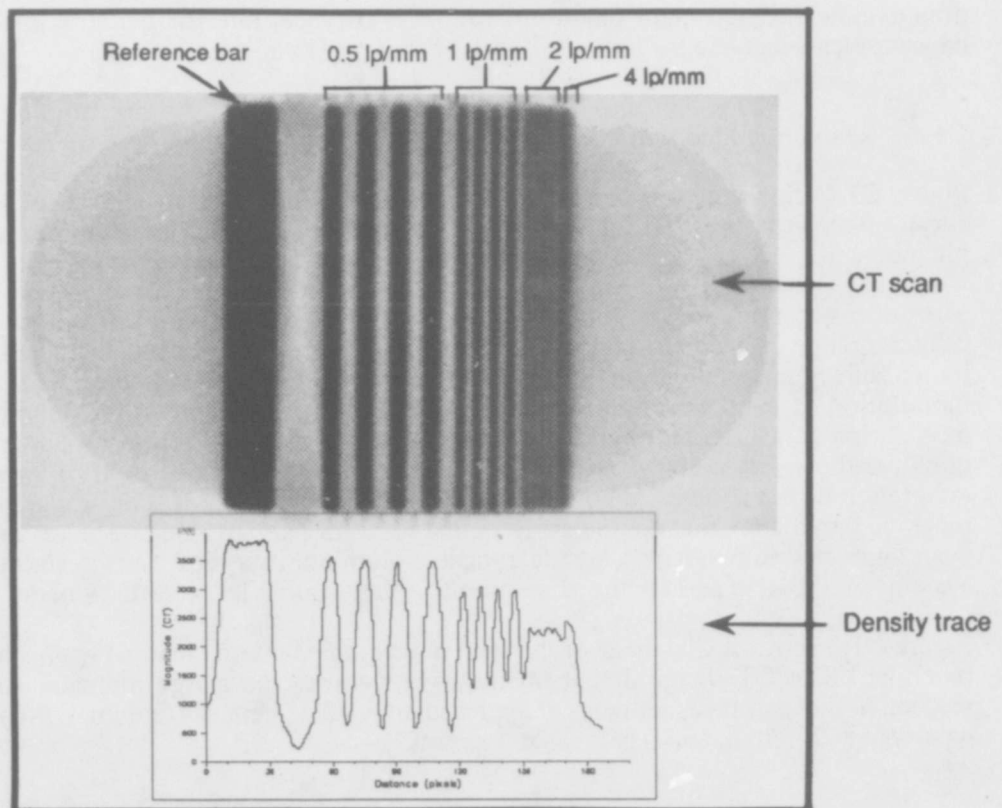


Figure C1-2 CT slice taken on the resolution phantom

## C2 Contrast Sensitivity Phantom

The contrast sensitivity phantom is a uniform disc of aluminum, 25 mm (1 inch) thick. Two sizes were made, one is 140 mm (5.5 inch) in diameter and the other is 70 mm (2.76 inch) in diameter. The smaller diameter size is used on systems with small fields of view or low kVp. Figure C2-1 shows an example CT slice of the large aluminum contrast sensitivity phantom with the corresponding density trace.

The measurement of contrast sensitivity is obtained by taking a region in the reconstructed image and determining the average and standard deviation for all CT numbers in the region. A typical region size of 1 cm (0.39 inch) diameter is used. Readings are usually taken at the center of the disk. The ratio of the average to the standard deviation is used as a signal to noise measurement. The inverse is a measure of contrast sensitivity. The signal to noise measurement for the density trace shown in Figure C2-1 is approximately 6.

The signal to noise ratio measurements are an important measure of system performance. The values improve with higher signal strengths. They also improve with smoothing algorithms in the reconstruction; however, this will decrease the resolution. Thus, the signal to noise and resolution must be considered together in assessing a quality level for performance.

## C3 Density Calibration Phantom

The density calibration phantom construction drawing is shown in Figure C3-1. It consists of an acrylic disk of 140 mm (5.5 inch) diameter with inserts of ten various materials.

The CT numbers for each insert from the reconstructed image are plotted against the known densities to serve as a calibration curve for the machine. The insert materials vary in atomic number which adds another variable in the process when the X-ray energy is such that the photoelectric effects are significant. Nevertheless, the phantom is useful for indicating the general density sensitivity and accuracy of a CT machine. A CT scan of the density calibration phantom is shown in Figure C3-2.

The calibration plot for a 420 kV CT system is shown in Figure C3-3. The CT number (or density), averaged over a small region in the center of the insert, is plotted along the horizontal axis and material density along the vertical axis.

## C4 Small Al Dimension Phantom

Figure C4-1 is a drawing of a small (40 mm (1.6 inch) diameter x 25 mm (1 inch) thick) aluminum dimension phantom. The phantom contains machined surfaces, bolted together to form gaps of 3, 1, 0.5, 0.25, 0.15 mm (0.12, 0.04, 0.02, 0.01, 0.006 inch) and both axial and side drilled holes of 3, 1 and 0.5 mm (0.12, 0.04, 0.02 inch) diameter. Figure C4-2 is a photograph of the phantom (PID #000801).

Dimensional measurement accuracy of a CT system will be a function of the resolution and contrast. Figure C4-3 shows a line trace taken across the 1 mm (0.04 inch) gap of the phantom from a CT system with approximately 10 percent modulation at 1 lp/mm and a signal-to-noise ratio of 70.

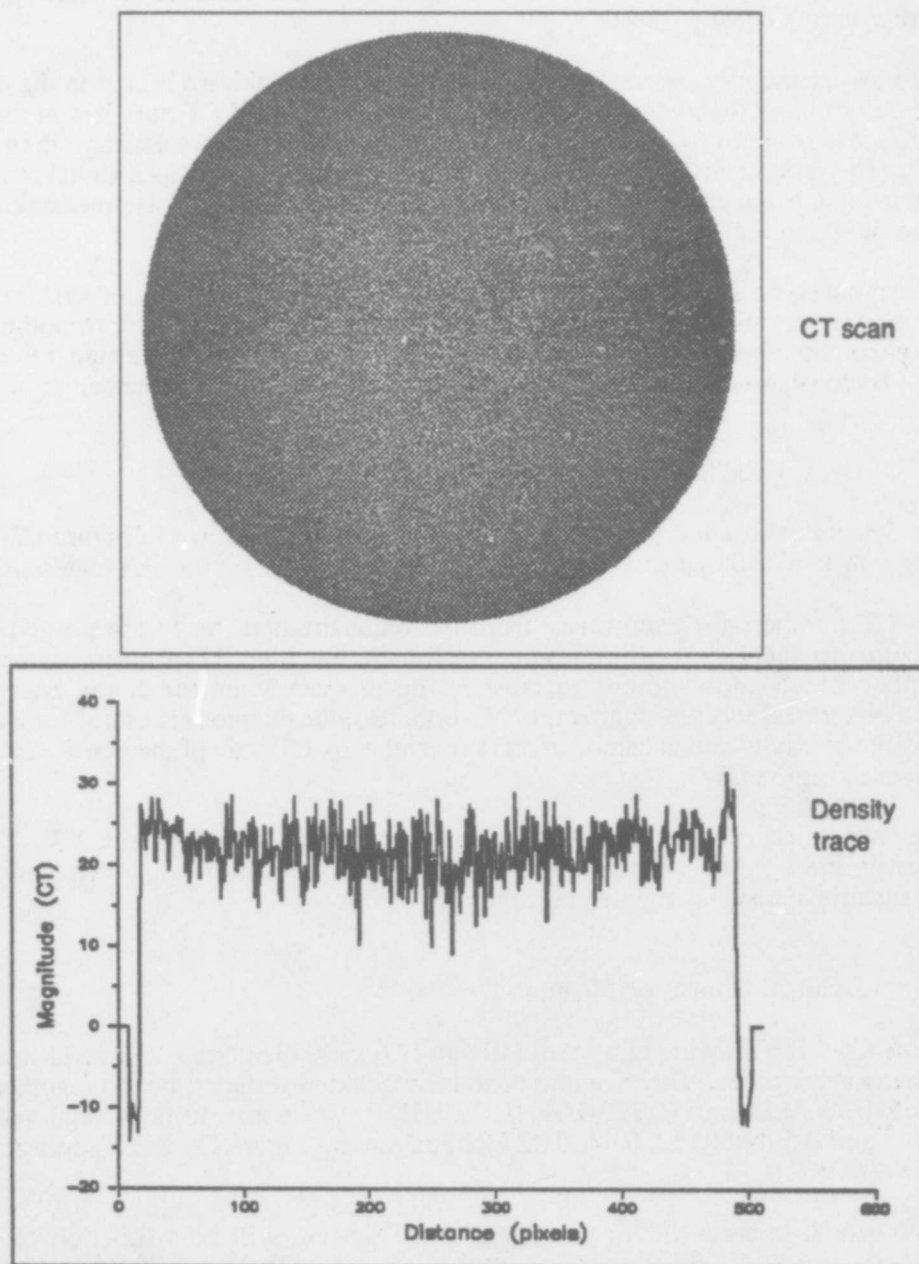
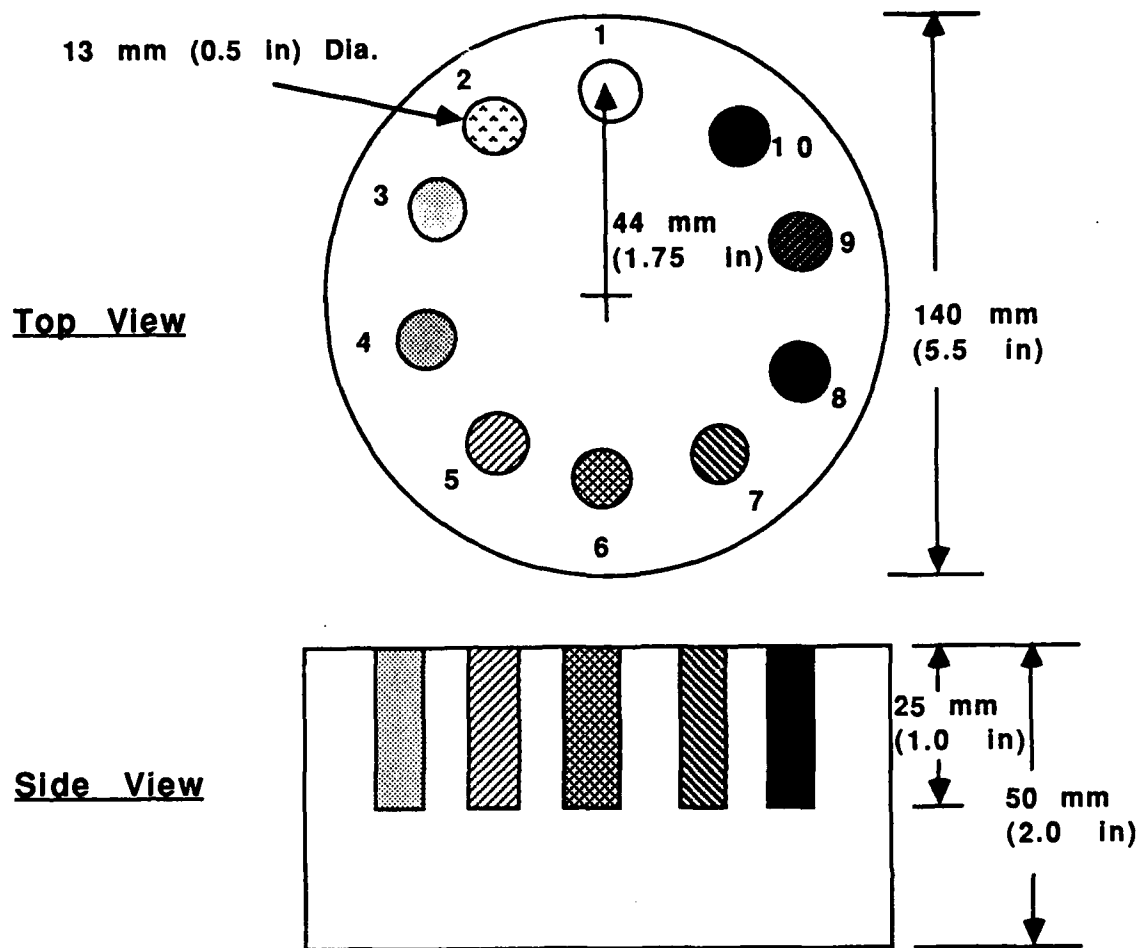


Figure C2-1 CT slice of contrast sensitivity phantom



Each density phantom is a cylinder measuring  
13 mm (.05 in) dia. x 25 mm (1.0 in) +/- .0025 mm (0.001 in)

The cylinders and their corresponding densities are listed below.

	<u>Material</u>	<u>Density (g/cc)</u>
1	Air Gap	
2	High Molecular Weight Polyethylene	0.945
3	Nylon	1.156
4	Nylatron	1.165
5	Acrylic Plexiglas (core material)	1.193
6	Delrin	1.507
7	Magnesium	1.784
8	Teflon	2.179
9	Aluminum	2.704
10	Titanium	4.423

Figure C3-1 Density calibration phantom

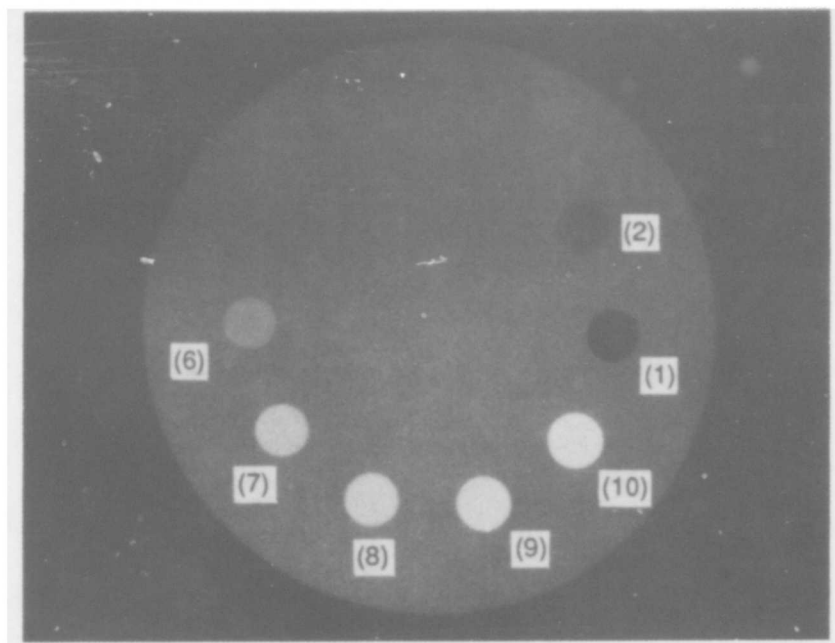


Figure C3-2 CT scan of density calibration phantom

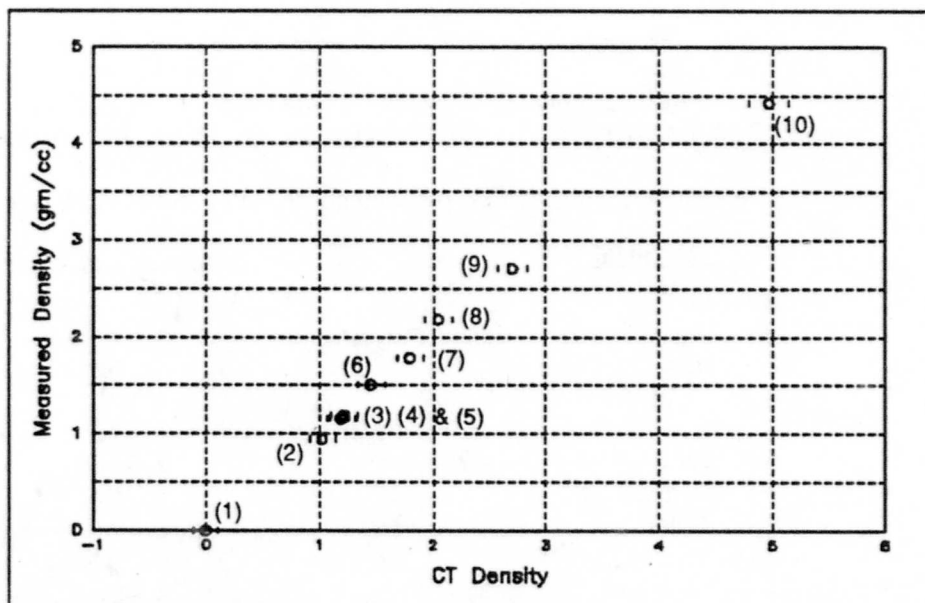


Figure C3-3 Calibration plot of density phantom

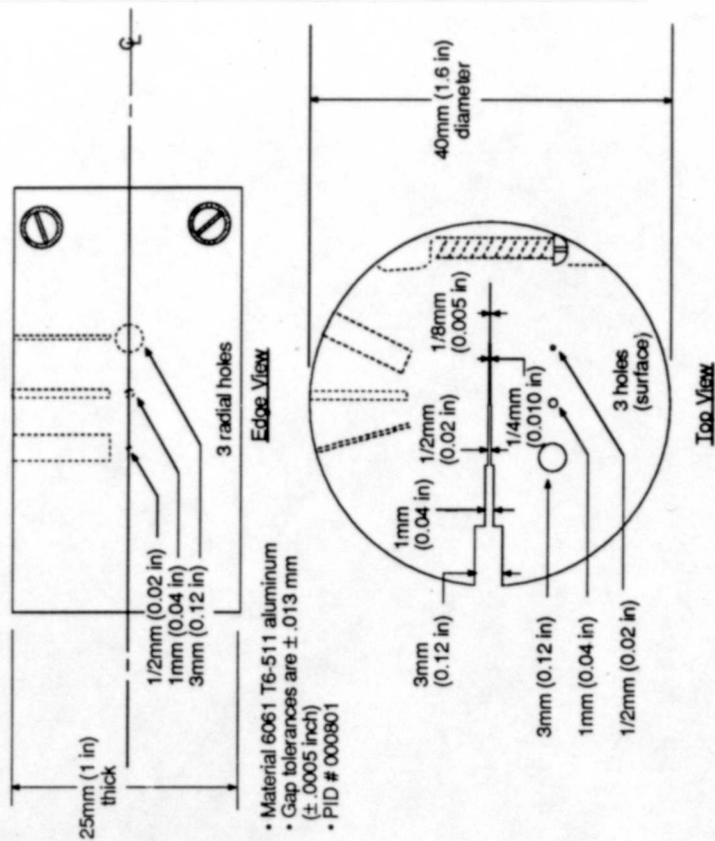


Figure C4-1 Aluminum dimensional phantom

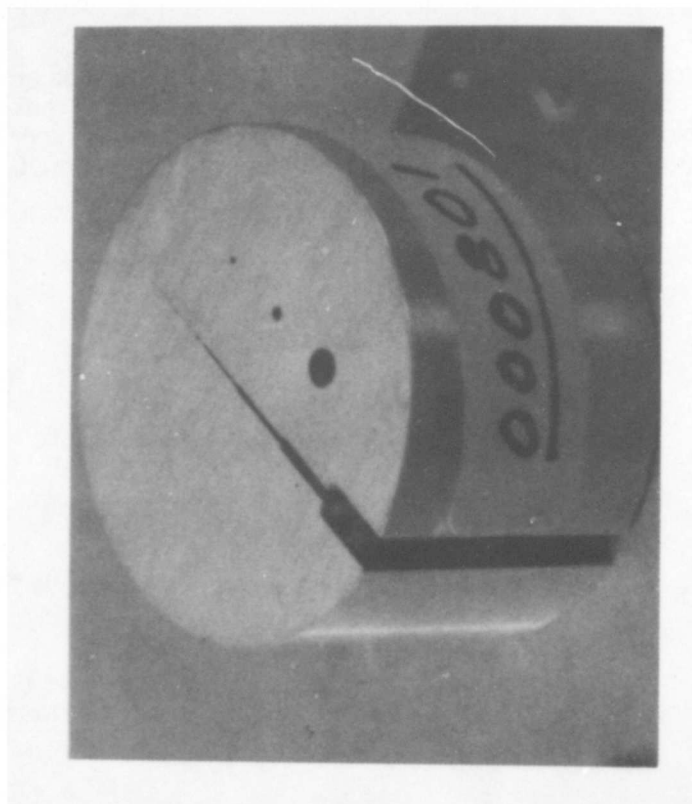
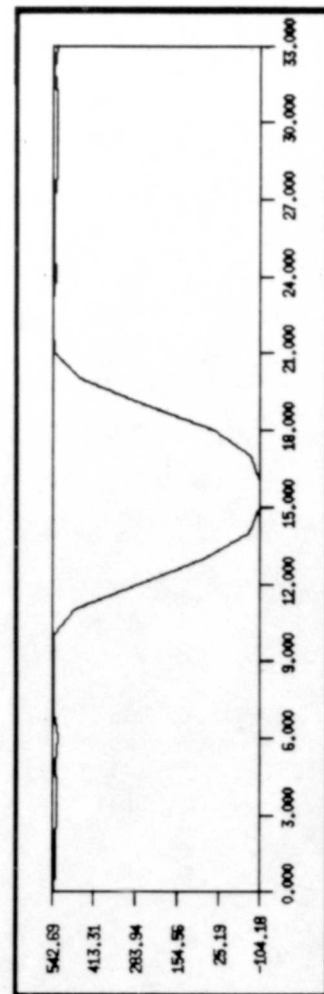


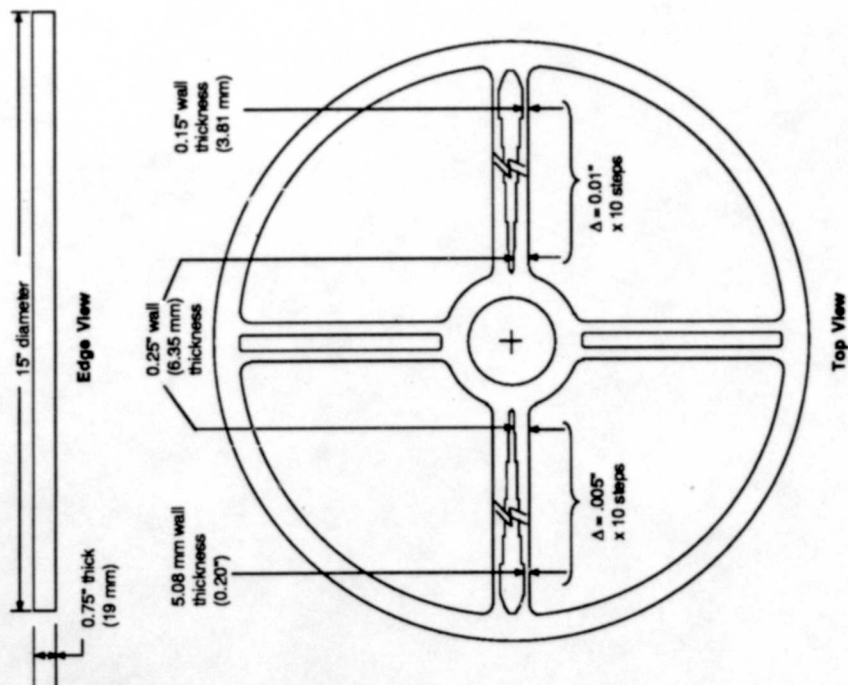
Figure C4-2 Photo of aluminum dimensional phantom



## C5 Large Dimension Phantom

Figure C5-1 is a drawing of a dimensional phantom that represents wall thinning in high alloy turbine engine parts. The material is steel. The 380 mm (15 inch) diameter phantom has spokes, two of which have thickness steps. One steps in units of 0.25 mm (0.01 inch) and the other in units of 0.125 mm (0.005 inch). Figure C5-2 is a photograph of the phantom (PID #000701). Figure C5-3 shows a line trace from a CT scan of the phantom to measure wall thickness.





- Material is 304 stainless steel (CPES)
- Gap tolerances are  $\pm 0.05"$  ( $\pm 0.13$  mm)
- PID # 000701

Figure C5-1 Steel dimensional phantom

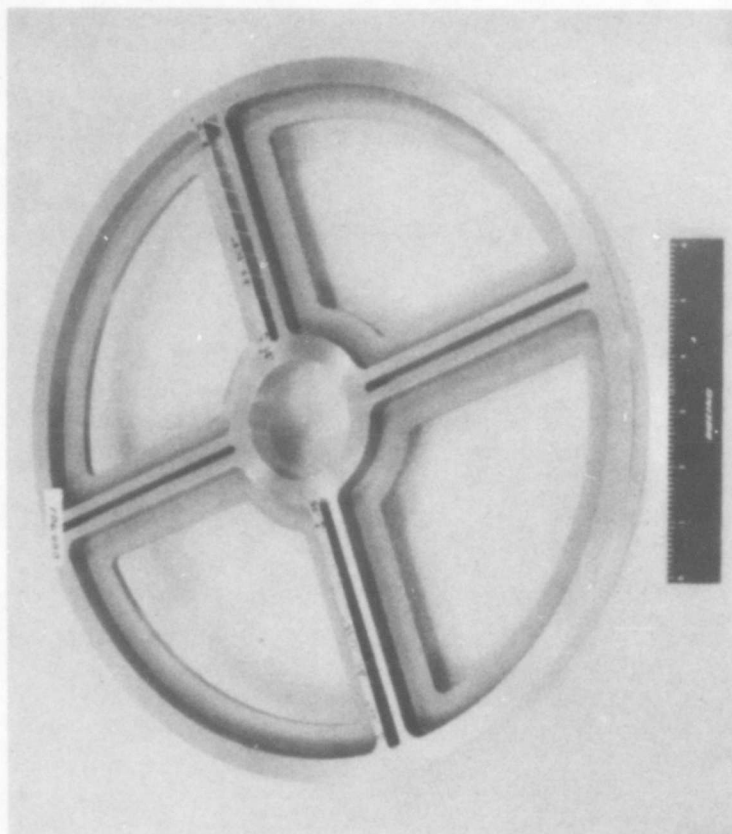


Figure C5-2 Photo of steel dimensional phantom

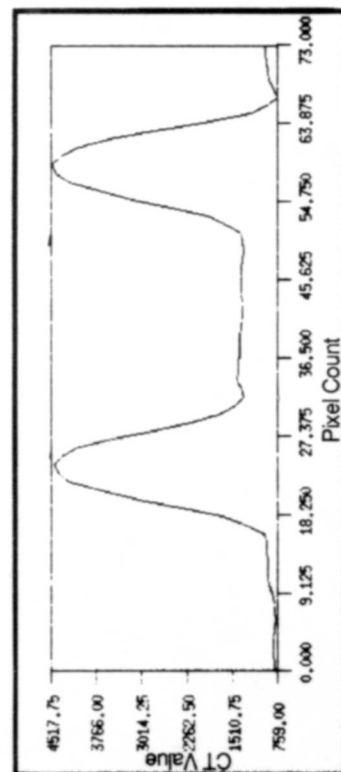


Figure C5-3 Line trace across spoke with two 3.8 mm walls